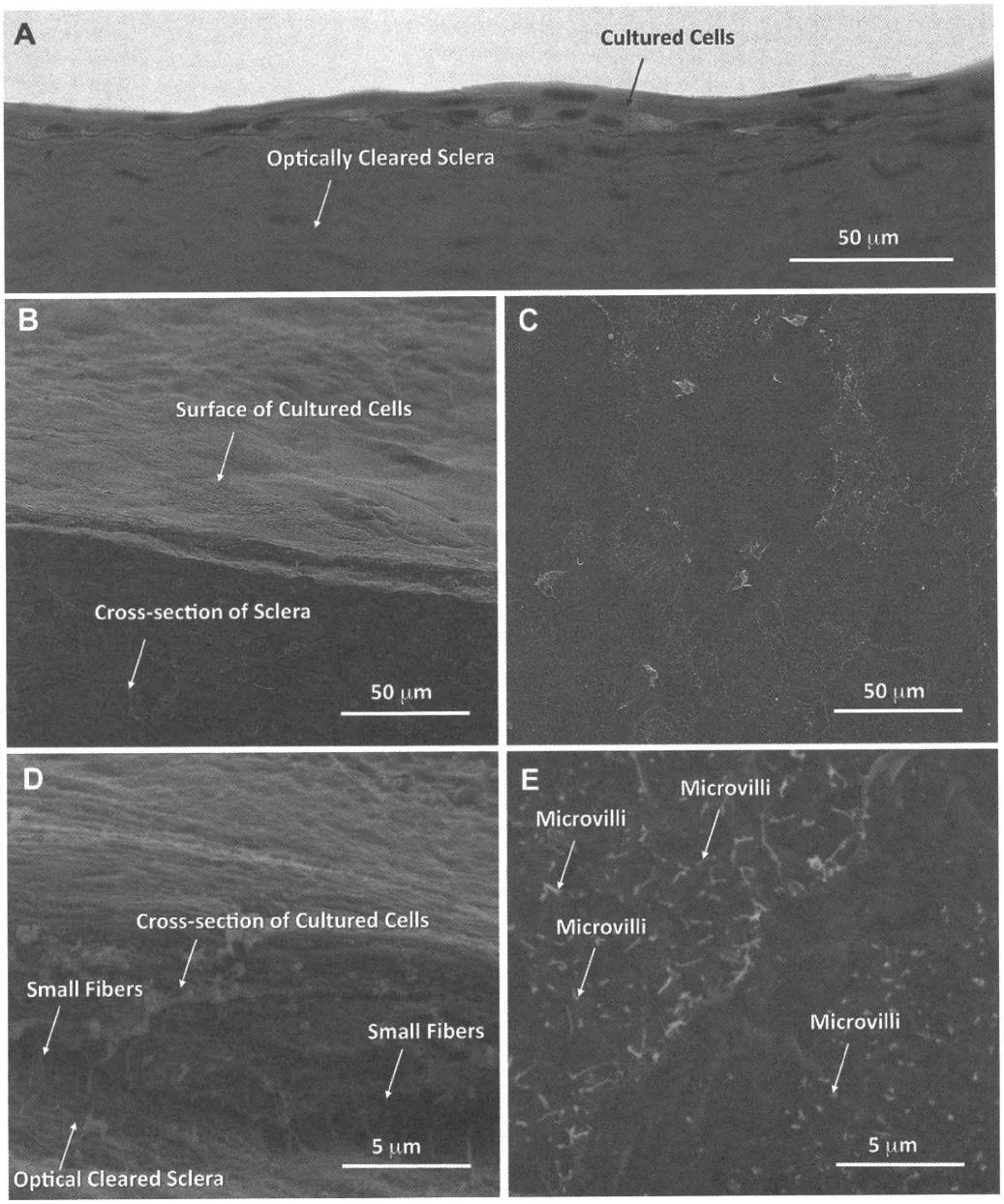


**Fig. 8.** Cultured rabbit corneal epithelial cells on irreversibly optically cleared sclera. HE staining of the cross-section (A), SEM images of the cross-section (B) and the flat mounted cell surface (C) at low-magnification, and images of the cross-section (D) and the flat mounted cell surface (E) at high-magnification.

process with 1% EDC/0.5% NHS was the best condition for providing the highest transmission to sclera and eliminating amounts of cross-linking reagent. When the concentration of EDC/NHS is high (10%/5%), the transparency significantly decreased with the possible structural distortion of sample.

The microscopical structure of the cross-section of sclera treated by the double-cycle treatment with 1% EDC/0.5% NHS was investigated by SEM after the critical point drying of the wet resultants (Fig. 6). This double-cycle treatment allowed the sclera thickness to be approx. 100 mm, which was less than 20% of the control sclera thickness without EDC and NHS (approx. 500 mm). In addition, the fiber structure in cross-linked rabbit sclera was observed to be much denser than that of non-cross-linked rabbit sclera.

On mechanical functional analysis, the double-cycle treated sclera with 1% EDC/0.5% NHS showed a sharper stress–strain curve in tensile test than that of native wet tissue (Fig. 7A). The applied stress at break point significantly increased by approx. 100% by this double-cycle treatment (Fig. 7B). In contrast, the strain at break point was significantly decreased by approx. 20% (Fig. 7C). In addition, the most illustrative change was found on the averaged Young's modules, which was significant increase by approx. 180% (Fig. 7D).

For investigating epithelial cell compatibility on the double-cycle treated rabbit sclera, seeded cells were rounded and floating, and the culture medium showed no color change for 3 days. In contrast, on arginine treated sclera, seeded epithelial cells proliferated and reached confluence with the color change of medium. After being cultured for 12 days, the regenerated epithelia on the sclera was fixed and analyzed. The light transmission of sclera was found to be stable during this cell culture experiments by visible inspection. Optical microscope and SEM showed that the surface of sclera was covered with 2–3 layered cells (Fig. 8A, B, and C). Morphology of the cultivated cell layer was flat and smooth at low magnification (Fig. 8B

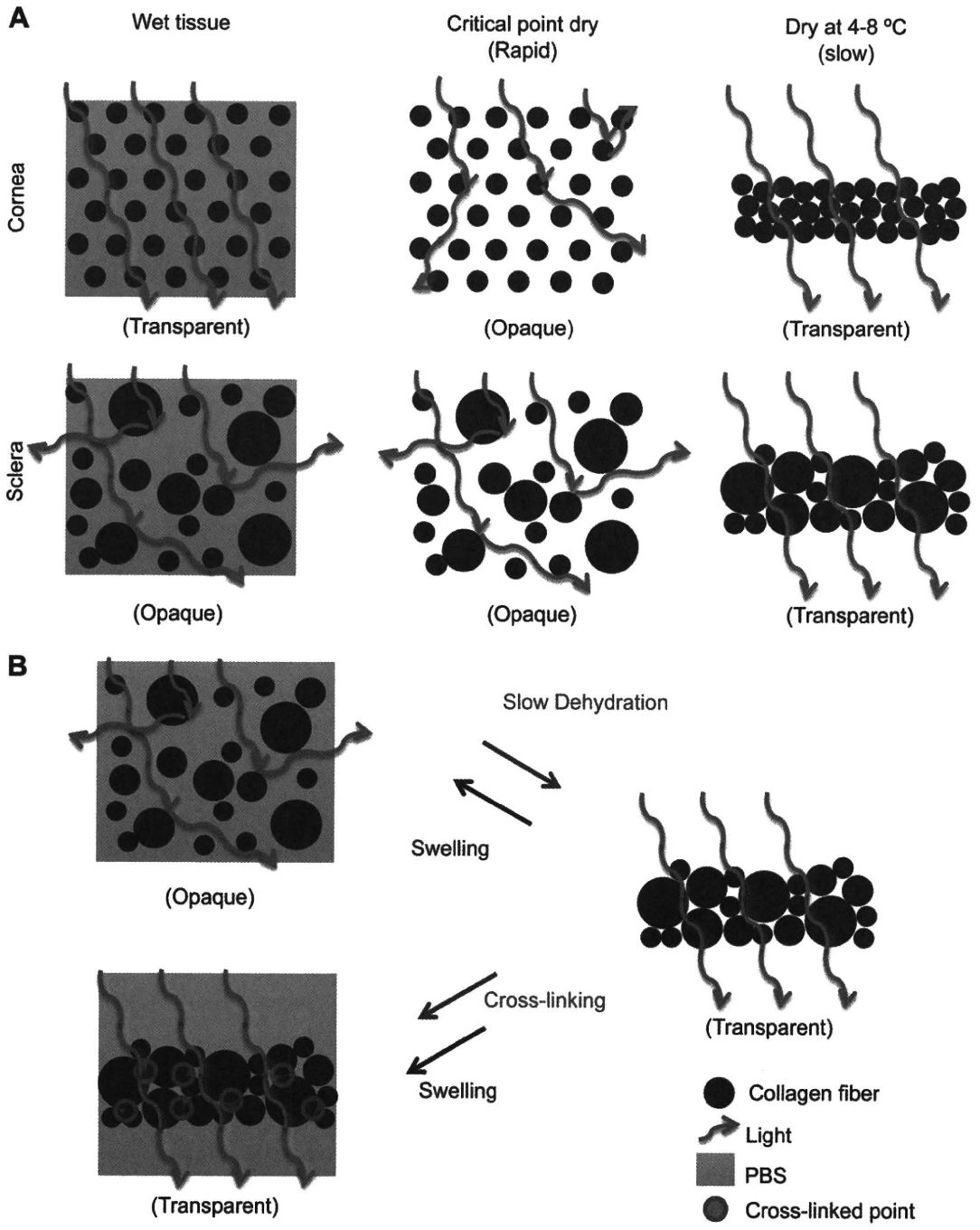


**Fig. 9.** Schematic illustration of structural effect on the transparency of cornea and sclera which were treated by low temperature dry or critical point dry (A), and collagen structure during the stabilization of transparency by chemical cross-linking (B).

and C). Small fiber-like structures (1–3 mm length), which connected cells and the surface of optically cleared sclera, were observed on the cross-section of the interface on the high-magnification imaging by SEM (Fig. 8D). Furthermore, microvilli were also observed on the surface of the cultured cells (Fig. 8E).

## 4. Discussion

Schematic illustrations of the proposed relationship between light transmission and structure in cornea and sclera, which were treated by two different dry processes, were given in Fig 9. Generally, the uniformity of fiber diameter and regularity of inter-fiber distance are considered to be essential for the regulation of visible-light transmission in cornea and sclera *in vivo* (the left column, Fig. 9A). Critical point drying is commonly used for dehydrating tissues with preserving their structures at wet condition, but treated cornea quickly lost its transparency (the first row and the middle column, Fig. 9A), because a stronger irregular light reflection occurs on the surface of collagen fibers in the tissues, which caused by large difference in refractive index between collagen ($n$ = 1.416) [7,18] and air ($n$ = 1.00) than that between collagen and water ($n$ = 1.333) in wet tissue. The high transparency obtained by low-temperature drying treatment (Figs. 1 and 2) may be strongly linked with the reduction of strong light scattering at

collagen–air interface in dense collagen packing (Fig. 3), with accompanying with fiber–fiber connection and inter-fiber space reduction (the right column, Fig. 9A). Such dense fiber packing is thought to be induced by capillary force during slow dehydration at low-temperature [19,20]. Speculations that the relationship between inner fiber packing and transparency are unrelated to the tissue-specific shapes of collagen fiber in cornea and sclera. The speculation is unable to contradict our results that showed that optically cleared cornea and sclera by low-temperature drying had a packed fiber structure that can transmit light (Fig. 1), and the speculation also supported the result of twice increase in transparency of dried rabbit sclera by eliminating irregular light reflection on its surface (Fig. 2).

Based on these results and discussion, the good visible-light transmission of wet chemically cross-linked sclera (Figs. 4 and 5) is caused by cross-linking adjacent fibers, which stabilize their dense fiber packing at wet condition (Figs. 6 and 9B). Repetition of low-temperature drying/chemical cross-linking with EDC/NHS (below 1%/0.5%) also reduced the inter-fiber spaces in the tissue. In addition, the repeated process also drastically reduced the necessary amount of cross-linking reagents for obtaining a high transparency over 50% at 550 nm by more than 90%. The maximum visible-light transmission of wet rabbit sclera obtained by the optimized multi-cycle treatment (Fig. 5) is higher than that of the rabbit sclera dried at low temperature without cover glass (Fig. 2) by 5–10%. This was probably caused by smaller light scattering at water–collagen interface than air–collagen interface on the surface and inside of the tissues with dense fiber packing.

In this study, the multi-cycle optical clearing successfully decreased the visible-light scattering of wet sclera. However, its maximum transparency was unable to be an optical level found in ocular application materials such as transplantable cell carriers [15,16,21–26] and replacement of corneal stroma [27–32]. The drastic reduction of light scattering and light reflection should be achieved for improving their optical property. The specific rigidity (a high Young's module) of this cross-linked sclera (Fig. 7) will provide a good stability in shape and light reflection to transparent tissue. On the other hand, a significant visible-light scattering probably occurs at the untreated rough surface of the wet tissue, and it is the same phenomenon found in dried rabbit sclera treated at low temperature with/without glass cover (Fig. 2). However, cover glass treatment was unsuitable for flatting the surface of wet tissues. Thus, special treatments are expected for obtaining a smooth surface on wet sclera such as excimer laser and micro-keratome treatments, in future study.

Another important function for clinical application is its biocompatibility. This study examined 4 chemical cross-linking reagents (Figs. 4 and 5) and UV irradiation treatment for cross-linking of tissue (Supporting Information 1). Mainly EDC and NHS were used, because they leaves no remain after their cross-linking reagents in their targeted sites. Therefore, no possible toxic substances release into tissues from subsequent cross-link breakdown [21,22,30,31,33,34], or they give no damage to collagen molecules. Observed cell toxicity without quenching reagent for cross-linking reagent caused by the un-reacted activated site and/or adsorbed reagents in the sclera. Arginine was used for quenching the cross-linking reaction and it's for improving cell adhesion [35]. Their efficacy of corneal epithelial cell culturing was successfully conformed. Obtained corneal epithelia cultured on the resultants were multilayered cell membranes with characteristic flat shape like corneal epithelial cells *in vivo* (Fig. 8), and the result indicated the transmission of components from feeder cells through the tissue. However, the thickness of the reconstructed epithelial cell layer was thinner, and the shape of cells on surface was broader than cultivated corneal/oral mucosal epithelium *in vitro* [25,36,37] and cornea *in vivo*. This will be one of our future works that should be studied by examining culture condition, the further modification of treatments of optically cleared sclera, etc.

The irreversibly optically cleared sclera exhibits a potential to use as a cell carrier and replacements for light transmission tissues. Also, our results indicated that the mechanisms of tissue optical clearing and developed method for irreversible optical clearing should be investigated on other tissues for further advance in tissue engineering as well as optical therapies/diagnosis.

## 5. Conclusion

This study found that dense fiber packing in dried tissue was a key for optical clearing of both cornea and sclera by two structural manipulations through dry processes. In addition, our cycle-treatments with low-temperature drying/chemical cross-linking successfully generate an transparent sclera, which was stable at wet condition. Irreversibly optically cleared sclera also exhibited a strong mechanical property and provided a scaffold character for corneal epithelial regeneration. The new optical clearing processes and the obtained transparent tissues have a potential for using in the field of tissue engineering and medicine, especially for ocular treatments.

## Acknowledgements

The authors are grateful to Prof. A. J. Quantock and Mr. T. Duncan of Cardiff University, Dr. K. Fukuyama of Meijigakuin University, and Dr. Y. Hatakeyama of Chiba University for their helpful discussion of structural analysis, and Dr. S. Dong and Miss Y. Sasaki of Tohoku University for their help. This work was financially supported by the Health and Labor Sciences Research Grants of Japan at Tohoku University, and Tohoku University Global COE for conquest of Signal Transduction Disease with "Network Medicine".

## Appendix

Figures with essential color discrimination. Figs. 7 and 9 in this article are difficult to interpret in black and white. The full color images can be found in the online version, at doi:10.1016/j.biomaterials.2010.10.002.

## Appendix. Supplementary data

Supplementary data associated with this article can be found, in the online version, at doi:10.1016/j.biomaterials.2010.10.002.

## References

[1] Moscoso M, Keller JB, Papanicolaou G. Depolarization and blurring of optical images by biological tissue. J Opt Soc Am A Opt Image Sci Vis 2001;18(4):948–60.
[2] Vargas G, Chan EK, Barton JK, Rylander 3rd HG, Welch AJ. Use of an agent to reduce scattering in skin. Lasers Surg Med 1999;24(2):133–41.
[3] Tuchin VV, Maksimova IL, Zimnyakov DA, Kon IL, Mavlutov AH, Mishin AA. Light propagation in tissues with controlled optical properties. J Biomed Opt 1997;2:401–17.
[4] Liu H, Beauvoit B, Kimura M, Chance B. Dependence of tissue optical properties on solute-induced changes in refractive index and osmolarity. J Biomed Opt 1996;1(2):200–11.
[5] Drew C, Milner TE, Rylander CG. Mechanical tissue optical clearing devices: evaluation of enhanced light penetration in skin using optical coherence tomography. J Biomed Opt 2009;14(6):064019.
[6] Rylander CG, Milner TE, Baranov SA, Nelson JS. Mechanical tissue optical clearing devices: enhancement of light penetration in ex vivo porcine skin and adipose tissue. Lasers Surg Med 2008;40(10):688–94.
[7] Doutch J, Quantock AJ, Smith VA, Meek KM. Light transmission in the human cornea as a function of position across the ocular surface: theoretical and experimental aspects. Biophys J 2008;95(11):5092–9.

[8] Meek KM, Fullwood NJ. Corneal and scleral collagens–a microscopist's perspective. Micron 2001;32(3):261–72.
[9] Freund DE, McCally RL, Farrell RA. Direct summation of fields for light scattering by fibrils with applications to normal corneas. Appl Opt 1986;25(16):2739.
[10] Maurice DM. The structure and transparency of the cornea. J Physiol 1957; 136(2):263–86.
[11] Ojeda JL, Ventosa JA, Piedra S. The three-dimensional microanatomy of the rabbit and human cornea. A chemical and mechanical microdissection-SEM approach. J Anat 2001;199(Pt 5):567–76.
[12] Titley KC, Smith DC, Chernecky R, Maric B, Chan A. An SEM examination of etched dentin and the structure of the hybrid layer. J Can Dent Assoc 1995;61 (10):887–94.
[13] Komai Y, Ushiki T. The three-dimensional organization of collagen fibrils in the human cornea and sclera. Invest Ophthalmol Vis Sci 1991;32(8):2244–58.
[14] Takushi E, Asato L, Nakada T. Edible eyeballs from fish. Nature 1990;345:298–9.
[15] Takezawa T, Ozaki K, Takabayashi C. Reconstruction of a hard connective tissue utilizing a pressed silk sheet and type-I collagen as the scaffold for fibroblasts. Tissue Eng 2007;13(6):1357–66.
[16] Takezawa T, Ozaki K, Nitani A, Takabayashi C, Shimo-Oka T. Collagen vitrigel: a novel scaffold that can facilitate a three-dimensional culture for reconstructing organoids. Cell Transplant 2004;13(4):463–73.
[17] Hayashida Y, Nishida K, Yamato M, Yang J, Sugiyama H, Watanabe K, et al. Transplantation of tissue-engineered epithelial cell sheets after excimer laser photoablation reduces postoperative corneal haze. Invest Ophthalmol Vis Sci 2006;47(2):552–7.
[18] Meek KM, Leonard DW, Connon CJ, Dennis S, Khan S. Transparency, swelling and scarring in the corneal stroma. Eye (Lond) 2003;17(8):927–36.
[19] Ciszek JW, Huang L, Tsonchev S, Wang Y, Shull KR, Ratner MA, et al. Assembly of nanorods into designer superstructures: the role of templating, capillary forces, adhesion, and polymer hydration. ACS Nano 2010;4(1):259–66.
[20] Kralchevsky PA, Nagayama K. Capillary interactions between particles bound to interfaces, liquid films and biomembranes. Adv Colloid Interface Sci 2000; 85(2–3):145–92.
[21] Tanaka Y, Kubota A, Matsusaki M, Duncan T, Hatakeyama Y, Fukuyama K, et al. Anisotropic mechanical properties of collagen hydrogels induced by uniaxial-flow for ocular applications. J Biomater Sci Polym Ed; 2010 [Epub ahead of print].
[22] Duncan TJ, Tanaka Y, Shi D, Kubota A, Quantock AJ, Nishida K. Flow-manipulated, crosslinked collagen gels for use as corneal equivalents. Biomaterials 2010;31(34):8996–9005.
[23] Helary C, Bataille I, Abed A, Illoul C, Anglo A, Louedec L, et al. Concentrated collagen hydrogels as dermal substitutes. Biomaterials 2010;31(3):481–90.
[24] Koizumi N, Sakamoto Y, Okumura N, Okahara N, Tsuchiya H, Torii R, et al. Cultivated corneal endothelial cell sheet transplantation in a primate model. Invest Ophthalmol Vis Sci 2007;48(10):4519–26.
[25] Nakamura T, Endo K, Cooper LJ, Fullwood NJ, Tanifuji N, Tsuzuki M, et al. The successful culture and autologous transplantation of rabbit oral mucosal epithelial cells on amniotic membrane. Invest Ophthalmol Vis Sci 2003;44(1): 106–16.
[26] Ng KW, Hutmacher DW. Reduced contraction of skin equivalent engineered using cell sheets cultured in 3D matrices. Biomaterials 2006;27(26): 4591–8.
[27] Carlsson DJ, Li F, Shimmura S, Griffith M. Bioengineered corneas: how close are we? Curr Opin Ophthalmol 2003;14(4):192–7.
[28] Griffith M, Osborne R, Munger R, Xiong X, Doillon CJ, Laycock NL, et al. Functional human corneal equivalents constructed from cell lines. Science 1999;286(5447):2169–72.
[29] Li F, Carlsson D, Lohmann C, Suuronen E, Vascotto S, Kobuch K, et al. Cellular and nerve regeneration within a biosynthetic extracellular matrix for corneal transplantation. Proc Natl Acad Sci U S A 2003;100(26):15346–51.
[30] Liu W, Deng C, McLaughlin CR, Fagerholm P, Lagali NS, Heyne B, et al. Collagen-phosphorylcholine interpenetrating network hydrogels as corneal substitutes. Biomaterials 2009;30(8):1551–9.
[31] Liu Y, Gan L, Carlsson DJ, Fagerholm P, Lagali N, Watsky MA, et al. A simple, cross-linked collagen tissue substitute for corneal implantation. Invest Ophthalmol Vis Sci 2006;47(5):1869–75.
[32] Rafat M, Li F, Fagerholm P, Lagali NS, Watsky MA, Munger R, et al. PEG-stabilized carbodiimide crosslinked collagen–chitosan hydrogels for corneal tissue engineering. Biomaterials 2008;29(29):3960–72.
[33] Marois Y, Chakfe N, Deng X, Marois M, How T, King MW, et al. Carbodiimide cross-linked gelatin: a new coating for porous polyester arterial prostheses. Biomaterials 1995;16(15):1131–9.
[34] Powell HM, Boyce ST. EDC cross-linking improves skin substitute strength and stability. Biomaterials 2006;27(34):5821–7.
[35] Massia SP, Hubbell JA. Immobilized amines and basic amino acids as mimetic heparin-binding domains for cell surface proteoglycan-mediated adhesion. J Biol Chem 1992;267(14):10133–41.
[36] Nishida K, Yamato M, Hayashida Y, Watanabe K, Maeda N, Watanabe H, et al. Functional bioengineered corneal epithelial sheet grafts from corneal stem cells expanded ex vivo on a temperature-responsive cell culture surface. Transplantation 2004;77(3):379–85.
[37] Nishida K, Yamato M, Hayashida Y, Watanabe K, Yamamoto K, Adachi E, et al. Corneal reconstruction with tissue-engineered cell sheets composed of autologous oral mucosal epithelium. N Engl J Med 2004;351(12):1187–96.

Biomaterials 31 (2010) 8996–9005

Contents lists available at ScienceDirect

Biomaterials

journal homepage: www.elsevier.com/locate/biomaterials

# Flow-manipulated, crosslinked collagen gels for use as corneal equivalents

Thomas J. Duncan [a,b,1], Yuji Tanaka [a,c,1], Dong Shi [a,d], Akira Kubota [a], Andrew J. Quantock [b], Kohji Nishida [a,*]

[a] Department of Ophthalmology and Visual Science, School of Medicine, Tohoku University, Sendai, Miyagi 980-8575, Japan
[b] Structural Biophysics Group, School of Optometry and Vision Sciences, Cardiff University, Cardiff CF24 4LU, Wales, United Kingdom
[c] Institute of Advanced Biomedical Engineering and Science, Tokyo Women's Medical University, Shinjuku, Tokyo 162-8666, Japan
[d] Department of Ophthalmology, The Fourth Affiliated Hospital, China Medical University, Shenyang 110005, China

ARTICLE INFO

*Article history:*
Received 14 July 2010
Accepted 19 August 2010
Available online 9 September 2010

*Keywords:*
Cornea
Collagen
Crosslinking
TEM (transmission electron microscopy)

ABSTRACT

Our aim was to construct a mechanically stable and optically transparent collagen gel from an acidified atelocollagen solution which is suitable for use as a corneal stromal equivalent. Light transmission and mechanical testing were conducted on variously crosslinked constructs at different pH levels. Ultrastructural analysis was performed to assess directionality of the molecular arrangement produced by flow manipulation, as well as the amount of collagen fibrillogenesis which resulted from different pH and/or crosslinking conditions. Clinical and histological integration of the gels with living tissue was examined following implantation into rabbit corneal intra-stromal pockets. Transmission electron microscopy revealed the importance of the fine control of pH levels during gel formation and indicated that the stage at which collagen fibrillogenesis is halted within the constructs was critically dependent on the pH of the collagen solution. Transparency testing disclosed that high levels of collagen fibrillogenesis, as well as high levels of crosslinker concentration, detrimentally affected the transparency of the construct. As a result, a dual titration was required to achieve good light transmission through the gels. It was also evident that the amount of crosslinking required to gelate the collagen solution was reduced as the level of fibrillogenesis progressed. Thus, it was necessary to establish a balance between the solution pH and crosslinker concentration. Implantation of the collagen constructs into partial depth intra-stromal pockets in rabbits was followed up for 6 months, and demonstrated favourable biocompatibility. This showed that gels which had lower levels of both fibrillogenesis and crosslinking were degraded more readily by the host tissue. The collagen gels described here are mass-production friendly, and have promise as potential functional stromal equivalents for use in stromal grafting, or in constructing full thickness artificial corneas.



## 1. Introduction

The cornea is the tough and precisely curved transparent window at the front of the eye which, aided by the crystalline lens in the eye's interior, focuses light onto the retina. The bulk of the cornea is made up of a collagen-rich stroma, bound either side by epithelial and endothelial cell layers. The corneal stroma possesses the mechanical strength needed to form the anterior outer coat of the eye, whilst still maintaining the high degree of transparency necessary for light transmission. Light transmission through the cornea is a result of a tissue-specific arrangement of uniformly thin collagen fibrils that measure approximately 30 nm in diameter in the hydrated state in man [1] (somewhat smaller when the tissue is fixed, dehydrated, embedded and observed in the electron microscope [2]). Collagen fibrils in the corneal stroma are arranged into a stacked array of about 250 layers or lamellae [3], which are thinner and more interwoven in the anterior cornea [4]. In humans the corneal stroma is approximately 500 μm thick [5], with commonly used experimental animal models having stromal thicknesses which vary from approximately 65–90 μm in mice (depending on the strain) [6,7], 450 μm in rabbit [8], and 800 μm in cow [9].

Theories of corneal transparency hold that the regular short-range spatial order in the collagen fibril array within each lamella allows for light transmission via interference effects [10–12]. This is evidenced by the opaque nature of the adjacent sclera – the white

* Corresponding author. Department of Ophthalmology, Osaka University Medical School, Suita, Osaka, Japan.
*E-mail address:* knishida@ophthal.med.osaka-u.ac.jp (K. Nishida).
[1] Equal contribution to this work.

0142-9612/$ – see front matter Crown Copyright © 2010 Published by Elsevier Ltd. All rights reserved.
doi:10.1016/j.biomaterials.2010.08.042

of the eye – which like cornea is a collagen-rich connective tissue, but with a less uniform fibril architecture. The characteristic collagen fibril arrangement in the cornea is believed to be maintained by the influence of different molecular subtypes within collagen fibrils [13], and by proteoglycan macromolecules which associate with the collagen and occupy the extrafibrillar space [9,14,15]. Collagen directionality in the plane of the cornea is also an important feature of the tissue, and is believed to affect the cornea's biomechanical stability [16]. Light scattering by cells called keratocytes, which occupy the stroma and which are interspersed between the collagen fibrils and lamellae, is minimized by the high concentration of water soluble proteins called transkeletolase and aldehyde dehydrogenase type I within the cells [17,18].

The arrangement of collagen has a key role in tissue function and the formation of a transparent and mechanically robust corneal stroma. However, the inherent complexity of the tissue's architecture has meant that it is difficult to produce effective constructs that mimic corneal structure and function [19,20]. For example, collagen fibril diameter, fibril spacing and fibrillar alignment, crucial for the mechanical and optical properties of the corneal stroma, would need precise regulation in order to successfully engineer a biomaterial that effectively resembles the stromal matrix and which has potential applications as a tissue substitute. At present this is difficult to achieve at the scale required for usable tissue construct size, although progress is being made [21].

As an alternative to generating a precisely ordered fibrillar structure, collagen gels have been investigated as possible corneal replacements. Over the last decade, scaffolds constructed from long collagen type I fibrils have been studied for use as potential stromal constructs [22–25]. Though highly biocompatible, these collagen

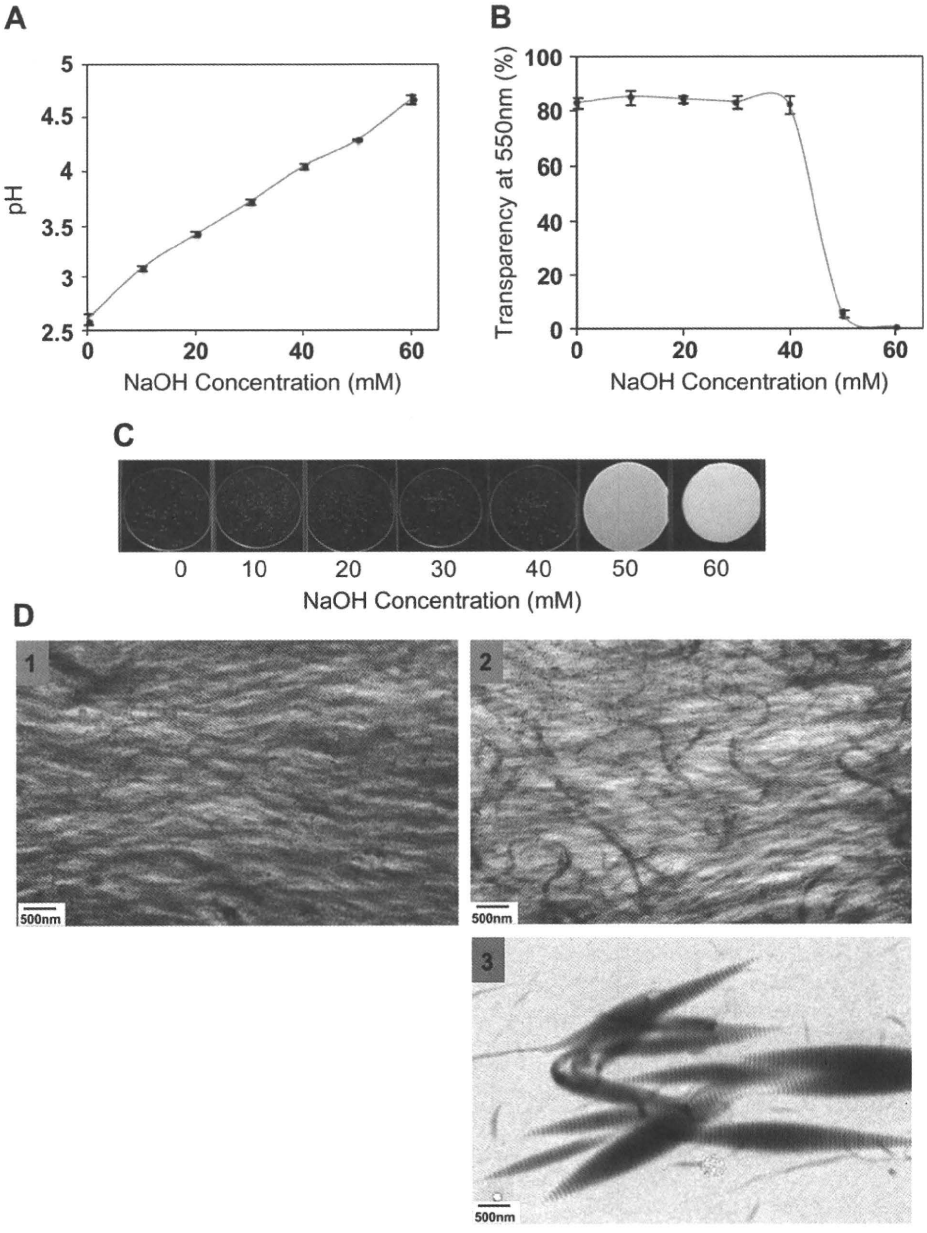


**Fig. 1.** Deacidification of a 10% (w/w) collagen solution through the addition of NaOH. (A) pH changes in the collagen solution upon NaOH addition. (B) Transparency changes in the collagen solution upon NaOH addition. (C) Photo image. (D) TEM images of collagen solutions using (1) 20 mM, (2) 40 mM, and (3) 60 mM of NaOH. The thickness of specimens in (A), (B) and (C) is 500 nm.

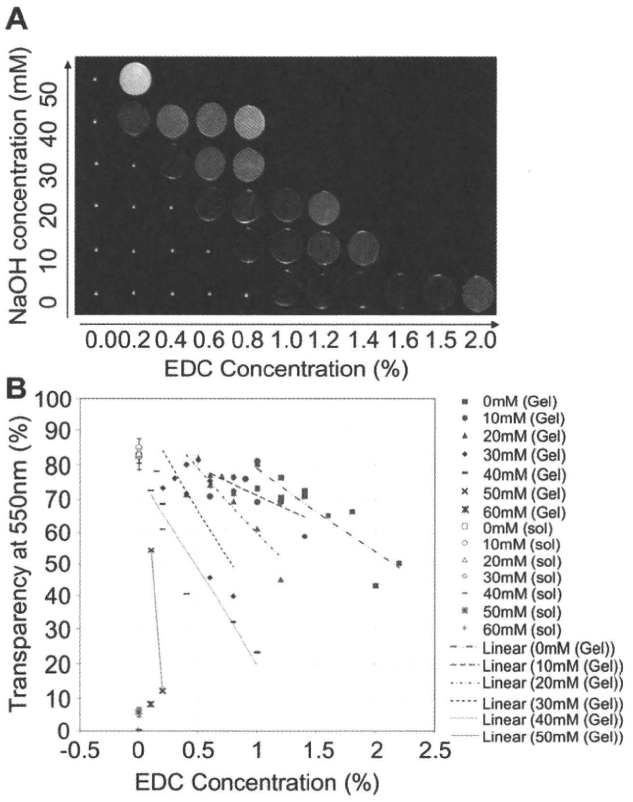


**Fig. 2.** Collagen gels formed by adding EDC/NHS crosslinking agents to deacidified collagen solutions. (A) Photo image and (B) transparency of collagen gels made using different NaOH and crosslinker levels. All samples are 500 μm thick, with a final collagen concentration of 10% (w/w), and a 2:1 weight ratio of EDC and NHS crosslinking agents. In (A) * denotes inadequate gel formation.

gels are often mechanically instable and have reduced transparency. The effect of including crosslinking agents or glycosaminoglycans on the mechanical and structural characteristics of collagen constructs has also been examined [26–29], although we are still a long way off being able to fabricate and modulate a fibrillar arrangement using proteoglycan additions. Little attention, however, has been paid to the structural and mechanical properties of type I collagen constructs formed at lower pH levels, the focus of this paper.

At high concentrations, type I collagen molecules will self assemble into a liquid crystalline array. By altering the conditions under which the construct is formed, it may be possible to produce a biocompatible tissue substitute which can accurately reproduce the structural and functional capabilities, though not the natural physiologic microanatomy, of the corneal stroma. In the current study we utilized atelocollagen, a telopeptide-free collagen molecule solution formed into a gel. To crosslink the gels, we applied a mixture of ethyl (dimethylaminopropyl) carbodiimide (EDC) and *N*-hydroxysuccimide (NHS) because these agents exhibit better biocompatibility and less toxicity than other crosslinkers such as glutaraldehyde. By manipulating the molecular assembly of highly concentrated atelocollagen solutions and optimizing the chemical environment, we were recently able to produce a transparent and mechanically stable crosslinked collagen gel using flow manipulation [30], which was well tolerated and incorporated into rabbit corneal stromas. The current study reports the transparency, ultrastructural directionality, bi-axial mechanical behavior and long term tolerance and integration into host tissue.

## 2. Materials and methods

### 2.1. Collagen solution and gel preparation

Acid freeze-dried type I porcine atelocollagen powder containing 5% type III collagen (Nippon Meat Packers) was dissolved at 4 °C in an HCl aqueous solution (pH 3.0) using a syringe mixing technique [31–34]. Centrifugation overnight at 3500 rpm was used to remove any air bubbles that were present. The pH of the collagen solution was then tuned to 3.5 by the addition, in an ice-water bath, of a NaOH 1.0 M aqueous solution using the same syringe mixing method. To create the gels, collagen solutions were mixed with a crosslinking solution of EDC/NHS (EDC:NHS = 2:1) until a homogeneous mixture was achieved. The final concentration of collagen was adjusted to 10% wet weight and that of EDC to 0.6% wet weight.

### 2.2. Collagen fibril alignment within the gel

Within 3 min of mixing the crosslinking agent with the collagen solution, 0.5 ml of the mixture was spread onto a glass slide in a 30 mm oval configuration. An elastic film was then placed on top, and a roller was used to spread the mixture in a unilateral direction. Silicon rubber spacers placed between the glass slide and the elastic film regulated the thickness of the gel to 500 μm. Incubation for 12 h at 20 °C and for 12 h at 37 °C was followed by PBS washing at 4 °C.

### 2.3. Transparency testing

500 μm thick collagen gels, or samples of non-crosslinked atelocollagen, were placed between two glass slides, separated by 500 μm thick silicon rubber spacers and held together with Parafilm. At room temperature, the transparency of the gels was measured using UV/vis-spectroscopy (UV-2550/2450, SHIMAZU, Japan) for narrow spectral regions centered at 400, 450, 500, 550, 600, 650, and 700 nm.

### 2.4. Mechanical testing

The mechanical characteristics of the collagen gels were tested in directions parallel to and at right angles to the direction of flow manipulation. The 500 μm thick gels were formed into dumb-bell shapes to prevent rupture at the point of attachment and to provide a larger area on which to attach the apparatus. A Universal Testing Instrument (EZ Test, SHIMADZU, Japan) was used at a rate of 100 mm/min to measure a rectangular region of the gels approximately 10 mm by 3 mm in size. The stress was measured as a function of strain, and by analyzing the linear region of the resulting stress-strain curve the elastic modulus of the constructs was calculated.

### 2.5. In vivo implantation

Three circular collagen gels with unilateral collagen orientation, 8 mm in diameter and approximately 135 μm thick were implanted into mid-depth stromal pockets of six male New Zealand White rabbits (2.0–3.5 kg; Kitayama Labs Co., Nagano, Japan). To achieve this, the rabbits were anesthetized intramuscularly with a mixture of ketamine hydrochloride (60 mg/kg; Sankyo, Tokyo, Japan) and xylazine (10 mg/kg; Bayer, Munich, Germany). A 6 mm-long circumferential incision was then made at the limbus and a stromal pocket created throughout the cornea at midstromal depth after which a rolled up gel was inserted and unfolded *in situ*. The following gels were implanted: 30 mM of NaOH with 0.8% EDC concentration, 30 mM of NaOH with 0.4% EDC concentration, and 10 mM of NaOH with 0.8% EDC concentration. The effect of the three different combinations of NaOH and crosslinker was assessed by histology and/or transmission electron microscopy at 1 and 6 months post-operative time points. An ultrasonic pachymeter used to measure the thickness of the cornea at regular intervals during the post-implantation period. Post-operatively, saline containing antibiotic medication was administered daily. All experimental procedures conformed to the ARVO (Association for Research in Vision and Ophthalmology) Statement for the Use of Animals in Ophthalmic and Vision Research and to local ethical rules.

### 2.6. Transmission electron microscopy

*In vitro* constructs and corneas which had been implanted with constructs up to the 6 month time point underwent the same processing routine, which involved immersion in a primary fixative containing 2.5% glutaraldehyde, 2% paraformaldehyde, and 1 M sodium cacodylate buffer for 3 h. En-bloc staining in 2% osmium textroxide and in 0.5% uranyl acetate for 1 h at room temperature was then followed by dehydration through a series of graded alcohols and propylene oxide, before embedding in Araldite resin. A Leica EM.UC6 ultramicrotome (Leica, Tokyo) was used to cut ultrathin sections (approx. 90 nm thick as assessed by the silver/gold interference colour), which were then mounted onto uncoated 200-square mesh copper grids. To analyze non-crosslinked collagen, a droplet of collagen in solution was wiped across the surface of a carbon-coated copper mesh grid. All grids were sequentially stained at room temperature, face down, on 25 μm droplets of 2% uranyl acetate, followed by 1% phosphotungstic acid with washes in between and after. A

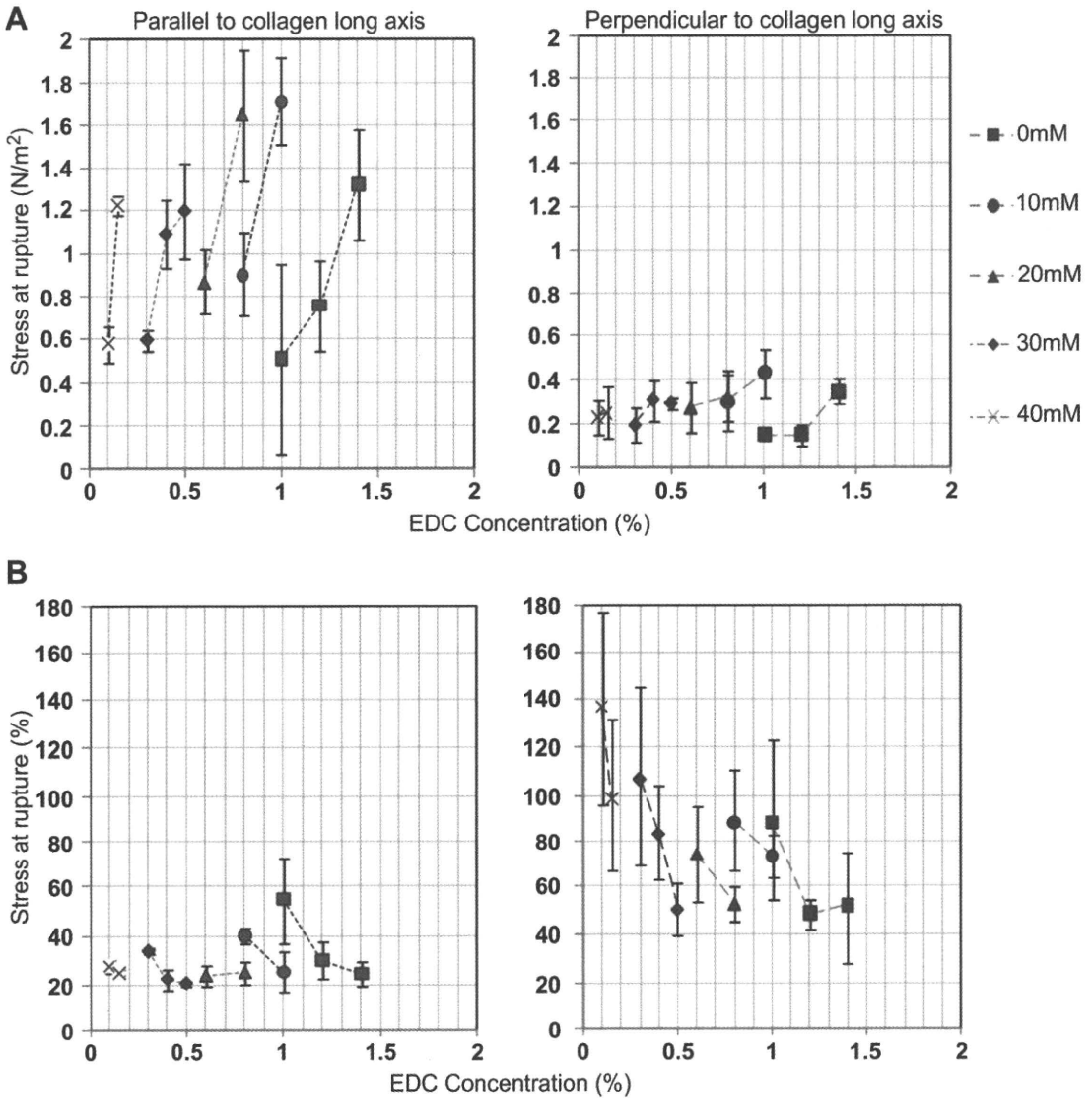


**Fig. 3.** Mechanical properties of collagen gels: (A) Stress measured in a direction parallel to and perpendicular to collagen alignment. (B) Strain measured in a direction parallel to and perpendicular to collagen alignment. Samples had transparency levels above 70%. All samples were 500 μm thick, with a final collagen concentration of 10% (w/w), and a 2:1 weight ratio of EDC and NHS crosslinking agents.

Hitachi H-7600 TEM (Hitachi, Japan) with a digital camera was used to image samples.

## 3. Results

Increasing the amount of NaOH used in the formation of the collagen solutions increased their pH, but reduced their transparency (Fig. 1). The effect on transparency was not linear however, with a clear step-change seen at NaOH levels above 40 mM. Below 40 mM of NaOH, transparency remained approximately constant at above 80% light transmission. An increase in NaOH concentration from 40 mM to 50 mM increased the pH of the solution from 4.05 to 4.29 – a relatively minor change – however, the effect on transparency was a profound, dropping from 82% to 6% light transmission (Fig. 1B). By 60 mM NaOH – the highest used in these experiments – pH was 4.66 and transparency measured less than 1%. At NaOH concentrations of 40 mM and below the collagen gels showed some directionality in flow manipulation. However, it was only at 60 mM of NaOH that any fibrils were formed that possessed the characteristic D-banding, and these resembled large tactoids reported by others [35,36] (Fig. 1D).

By crosslinking the collagen solution, a gel could be produced. It is clear from Fig. 2 that as NaOH levels increase, transparency of the gel decreases similar to the effect on collagen solutions shown in Fig. 1. Increasing the levels of crosslinking also reduces the transparency of the gel. Consequently, as the amount of NaOH was increased in the gels, the amount of crosslinking needed to be reduced accordingly in order to keep desirable levels of transparency (Fig. 2). Crosslinking the collagen solutions, as expected, had the effect of improving their mechanical stability, increasing their tensile strength and decreasing the strain at rupture (Fig. 3). All gels tested for mechanical stability had transparency levels above 70%. Concurrent with the transparency data presented in Fig. 2, at higher NaOH levels less crosslinking was required to produce a mechanically stable gel. For example, similar stress levels at rupture were seen in gels made with 30 mM NaOH and 0.5% EDC concentration, as well as in gels made with 40 mM NaOH but which had received only 0.15% EDC. The improvement in mechanical

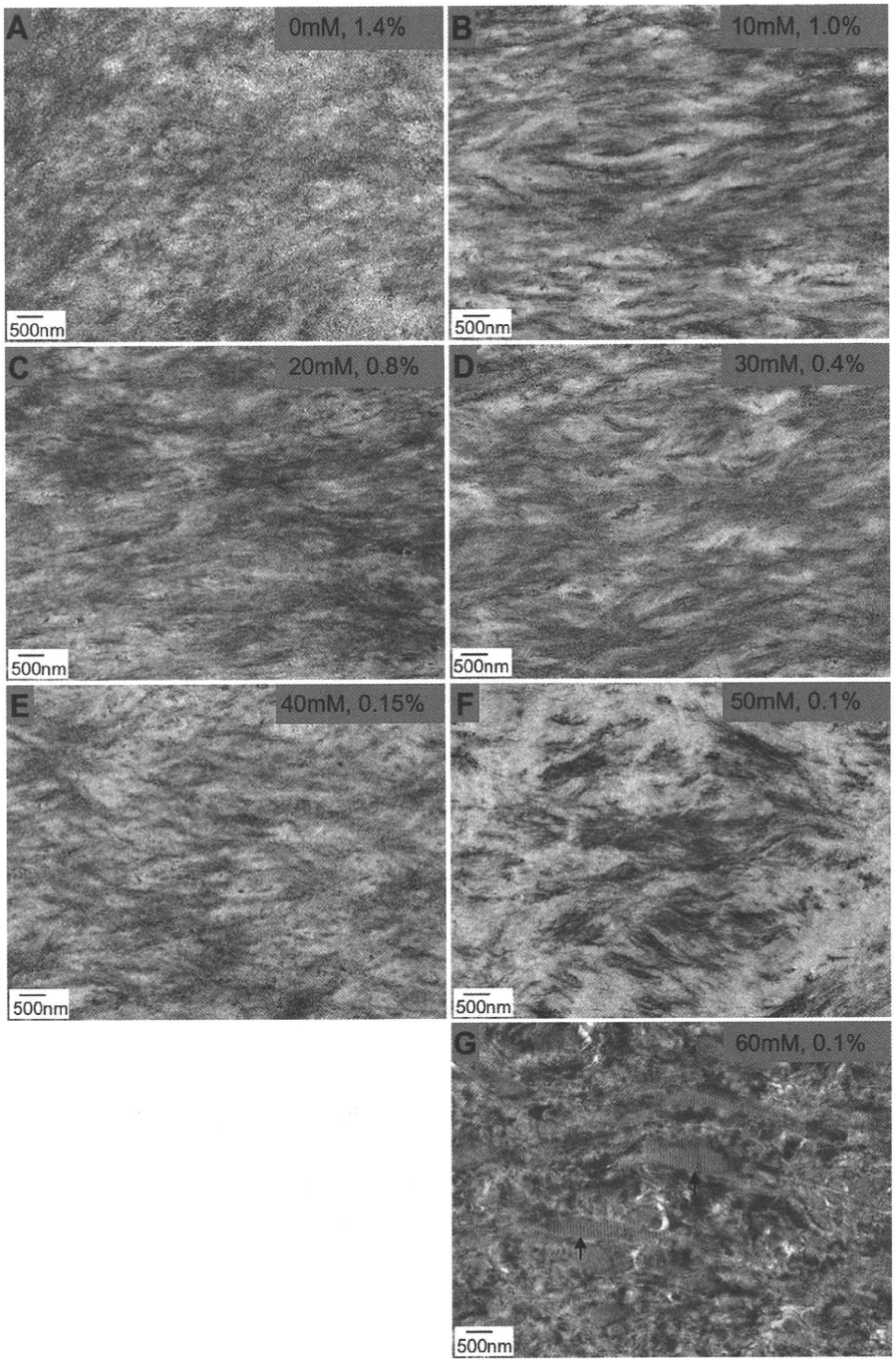


**Fig. 4.** TEM images of collagen gels at ×3500 magnification. All samples were 500 μm thick. Gel conditions are (A) 0 mM NaOH, 1.4% EDC/NHS (B) 10 mM NaOH, 1.0% EDC/NHS (C) 20 mM NaOH, 0.8% EDC/NHS (D) 30 mM NaOH, 0.4% EDC/NHS (E) 40 mM NaOH, 0.15% EDC/NHS (F) 50 mM NaOH, 0.1% EDC/NHS (G) 60 mM NaOH, 0.1% EDC/NHS. Black arrows in micrograph indicate tactoids.

strength that accompanied crosslinker addition responded to smaller rises in crosslinker percentage as NaOH levels were increased. For example, 0 mM NaOH gels showed a close-to-doubling in tensile strength (from 0.75 $N/m^2$ to 1.32 $N/m^2$) when the crosslinker concentration was increased by 0.2%. However, in 40 mM NaOH gels, a similar magnitude rise in tensile strength (from 0.57 $N/m^2$ to 1.22 $N/m^2$) was achieved through just a 0.05% increase in crosslinker concentration (Fig. 3). This data also implies that a uniaxial alignment of collagen during gel formation using the flow manipulation approach influences the mechanical behavior of the constructs. For example, the tensile strength of gels tested was approximately three fold higher in a direction parallel to the axis of the collagen than in the perpendicular direction. Strain levels, moreover, were approximately doubled when tensile loading was applied in a direction at right angles to the collagen long axis, than when loaded along the collagen axis. Using increased levels of crosslinker reduced the level of strain at rupture, whilst higher levels of NaOH caused greater levels of strain (Fig. 3).

Transmission electron micrographs of the gels were taken at each different NaOH condition used: 0 mM, 10 mM, 20 mM, 30 mM,

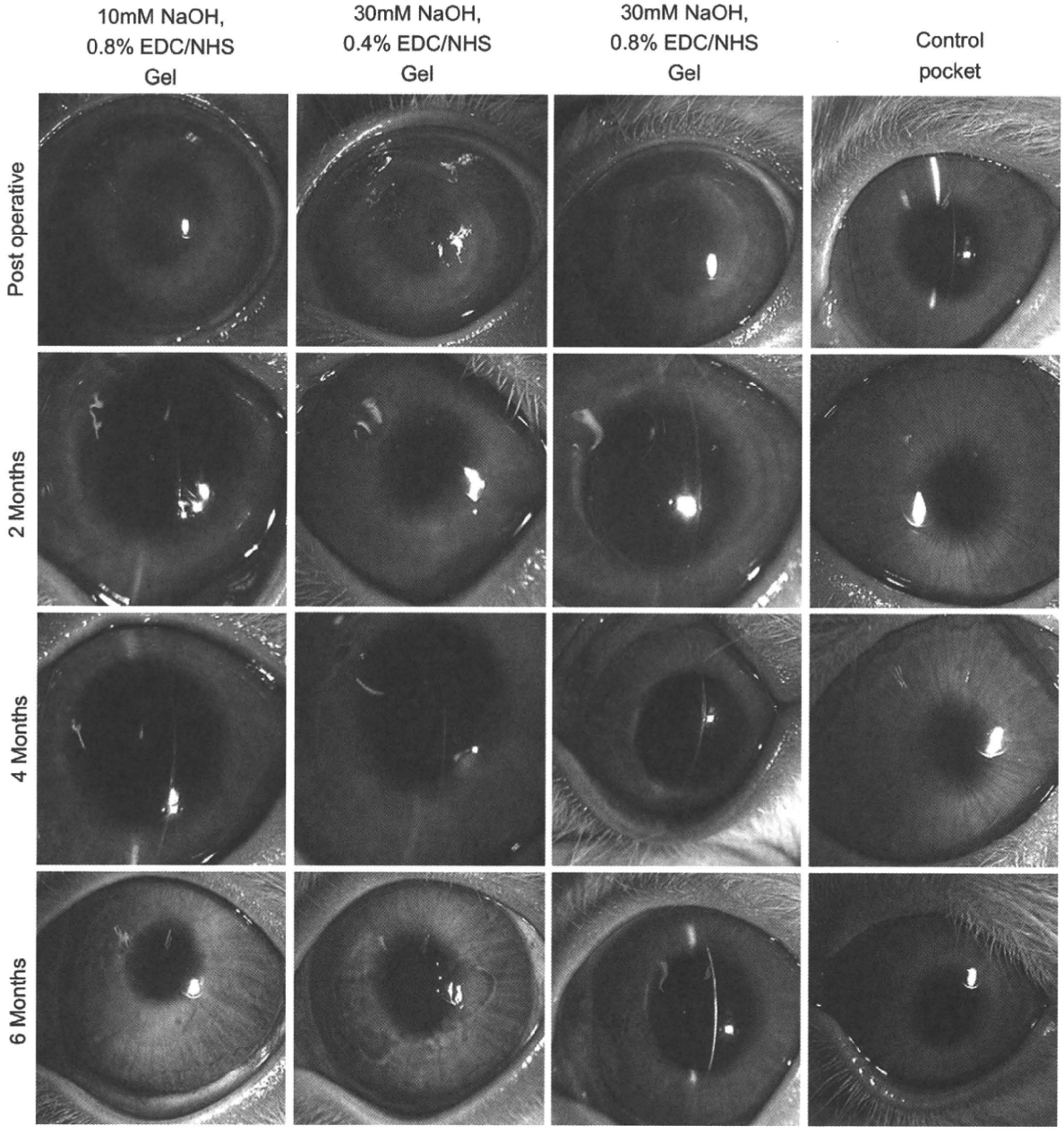


**Fig. 5.** Six month implantation of collagen gels into rabbit intra-stromal pockets. Collagen gel dimensions were 8 mm in diameter and 100–200 μm in thickness.

40 mM, 50 mM and 60 mM. This revealed that as NaOH levels increased there was a progressive condensation of the collagen within the gel into progressively longer filamentous structures (Fig. 4). At pH 2.6 (i.e. with 0 mM of NaOH) the collagen was present in the gel as a loose matrix with little clear ultrastructure. Increasing the pH to 3.08 using 10 mM of NaOH resulted in the formation of aggregates or bundles of collagen with a clear directionality because of the flow manipulation used in the gel manufacture and which is manifest in preferential strength along the axis of the collagen. Repeated addition of 10 mM NaOH increased the pH of the gels to 3.42, 3.73 and 4.05, respectively. This resulted in the formation of increased levels of aggregation (Fig. 4), and at a pH of 4.29 using 50 mM of NaOH the collagen was organized into more compact bundled structures than was the case for the 30 mM or 40 mM NaOH gels (Fig. 4). More mature fibrils, demonstrating a characteristic D-periodicity banding pattern, could only be seen in gels made with 60 mM of NaOH, as was the case for the collagen in solution (Fig. 1D).

Collagen gels made with different NaOH/crosslinker combinations are all well tolerated when implanted into mid-depth rabbit corneal intra-stromal pockets with no sign of inflammation or rejection. The three different gel types all show good biocompatibility and transparency up to 6 months post-operatively (Fig. 5). In the immediate post-operative period the thickness of the operated corneas measured by ultrasonic pachymetry (Fig. 6) is significantly increased due to a combination of the addition of extra material in the stroma and to the intrusive nature of the surgical procedure itself – i.e. the sham operated pocket-only cornea is approximately 150 μm thicker after surgery indicating that the stroma does not immediately revert to normal. One week after surgery, however, the control surgical cornea has returned to near normal thickness, whereas the implanted corneas all remain significantly thicker than

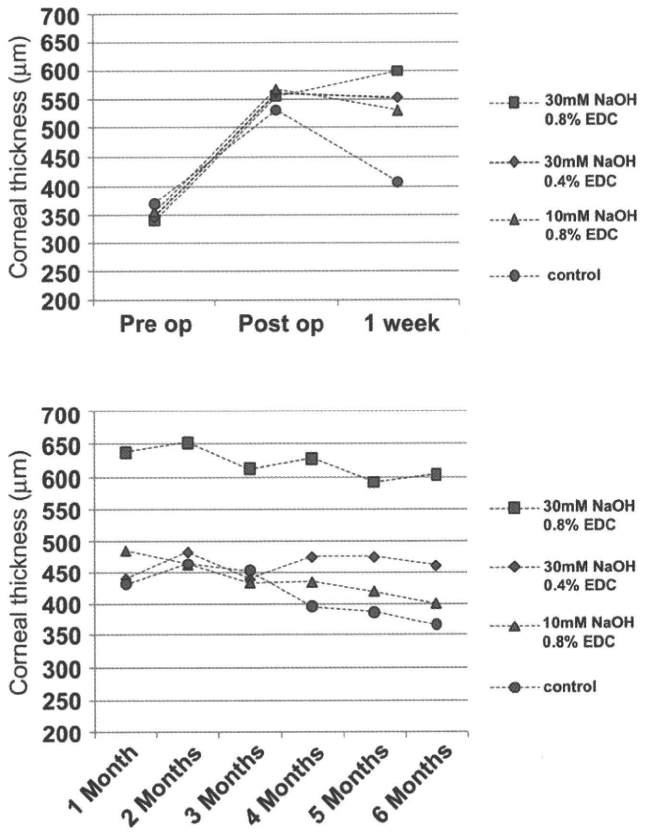


**Fig. 6.** Rabbit corneal thickness measurements following implantation of collagen gels into midstromal rabbit pockets. Collagen gel dimensions were approximately 8 mm in diameter.

pre-implant values (Fig. 6A). A subsequent reduction in corneal thickness of the construct-implanted corneas over the following several months suggests that there may be some incorporation, remodeling or digestion of the gels by the host tissue. It was notable from the thickness measurements, however, that the 30 mM NaOH gel crosslinked with 0.8% EDC appears to have resisted the digestion more than the other gel types over the implantation period.

The incorporation, remodeling or digestion of implanted gels was confirmed by histological analysis (Fig. 7). In all cases, the 30 mM NaOH, 0.8% EDC/NHS gel was prominent in the host tissue, even 6 months after implantation. Moreover, some oedema seems to have occurred in the anterior region stroma above this implant by this time point possibly due to a restriction in the diffusion of metabolites through the stroma. The 30 mM NaOH, 0.4% EDC/NHS gel is still evident in the stroma 6 months post-implantation, but no anterior stromal oedema seems to have occurred in this case. The 10 mM NaOH gel was the least retained of the gels tested, with minimal gel remaining 1 month after implantation.

TEM analysis of the implanted gels *in situ* showed that the invasion of host cells into the gels was often accompanied by remodeling or digestion of the gels (Fig. 8). Despite the gels being crosslinked during their fabrication, their morphological appearance changed after prolonged placement within the host tissue. A relatively high level of collagen fibril formation could be seen in the 30 mM/0.8% gel after 6 months of implantation compared to the 1 month time point, suggestive of a progression in fibrillogenesis during the implantation period. Similar to the results seen in Fig. 4, the morphological properties of the gels *in situ* does vary depending on the ratio and amounts of NaOH and crosslinkers used during their production – with lower NaOH and crosslinker levels producing a gel with a less well defined matrix of more loosely associated collagen filaments. In agreement with histological observations (Fig. 7), the 10 mM NaOH, 0.8% EDC/NHS gel was not observed in the stroma at the time of sacrifice. Only at 1 month post-implantation could any remnants of this gel be found under TEM analysis (Fig. 8). Cellular infiltration was also more prevalent in the 10 mM/0.8%, and 30 mM/0.4% gels.

## 4. Discussion

The data presented here shows the critical importance if producing a suitable chemical environment if we are to fabricate a functional and implantable gel-like biomimetic collagen construct for use in corneal surgery. The changes in light transmission in the collagen solutions with varying pH demonstrate that a critical point is reached just above pH 4.0, after which the pH has a highly detrimental effect on the transparency of the collagen solutions. A similar pattern of reduced light transmission with higher NaOH levels was seen for the crosslinked collagen gels, but in this case the situation was less straightforward because at identical pH levels, light transmission was differently affected depending on the amount of chemical crosslinker used. Not inducing sufficient crosslinking, however, would result in a mechanically unstable gel, thus it was necessary to find a balance between these two factors in order to produce a robust, flexible and usable transparent gel. Based on these initial experiments, gels judged to be potentially suitable for grafting into living tissue were chosen as 30 mM NaOH with 0.8% EDC, 30 mM NaOH with 0.4% EDC, and 10 mM NaOH with 0.8% EDC.

Crosslinking, as expected, enhanced the mechanical strength of the collagen gels – improving tensile strength in a direction parallel to collagen alignment, and improving the elastic properties of the gels in a perpendicular direction. Interestingly, the elastic properties of the gels parallel to the flow direction were found to be similar to those of human corneal tissue ($3.81 \pm 0.40$ N/mm$^2$ in tensile strength [37], 3–13 N/mm$^2$ in Young's modulus [38]).

Constructs formed under increasingly basic conditions demonstrated greater stress and strain levels at rupture in both the plane parallel to, and the plane perpendicular to, the collagen axis. The observation that the stress–strain relationship is a function of pH has been reported in numerous other studies involved collagen hydrogels [39,40]. In these published studies, the length and diameter of the forming collagen fibrils, along with their organization, had a dramatic impact on the mechanical properties of the constructs. For example, Parry has shown that increased levels of small diameter collagen fibrils protect tendon tissue structure from plastic deformation [41]. Roeder and associates have also reported that an increased pH had the effect of increasing fibril length and decreasing fibril diameter, which in turn improved the mechanical properties of the collagen matrices [40]. It has been suggested that fibril length has a greater influence on the viscoelastic properties than does fibril diameter [40,41]. In particular the longitudinal fusion of fibril subunits increases the resistance to high strain level deformation. The lateral fusion of fibril subunits also has an impact on mechanical properties, but this was found to be specific to low strain level deformation resistance [39].

TEM images of the gels produced here show that the diameter of the condensing collagen structures appears to decrease as pH increases. Research by others which has focused on the later stages of fibril assembly at higher pH levels, have also observed similar results [39,42]. In our micrographs a range of subfibrillar intermediates could be identified - from a largely disorganized matrix of collagen molecules, through intermittent molecular aggregations,

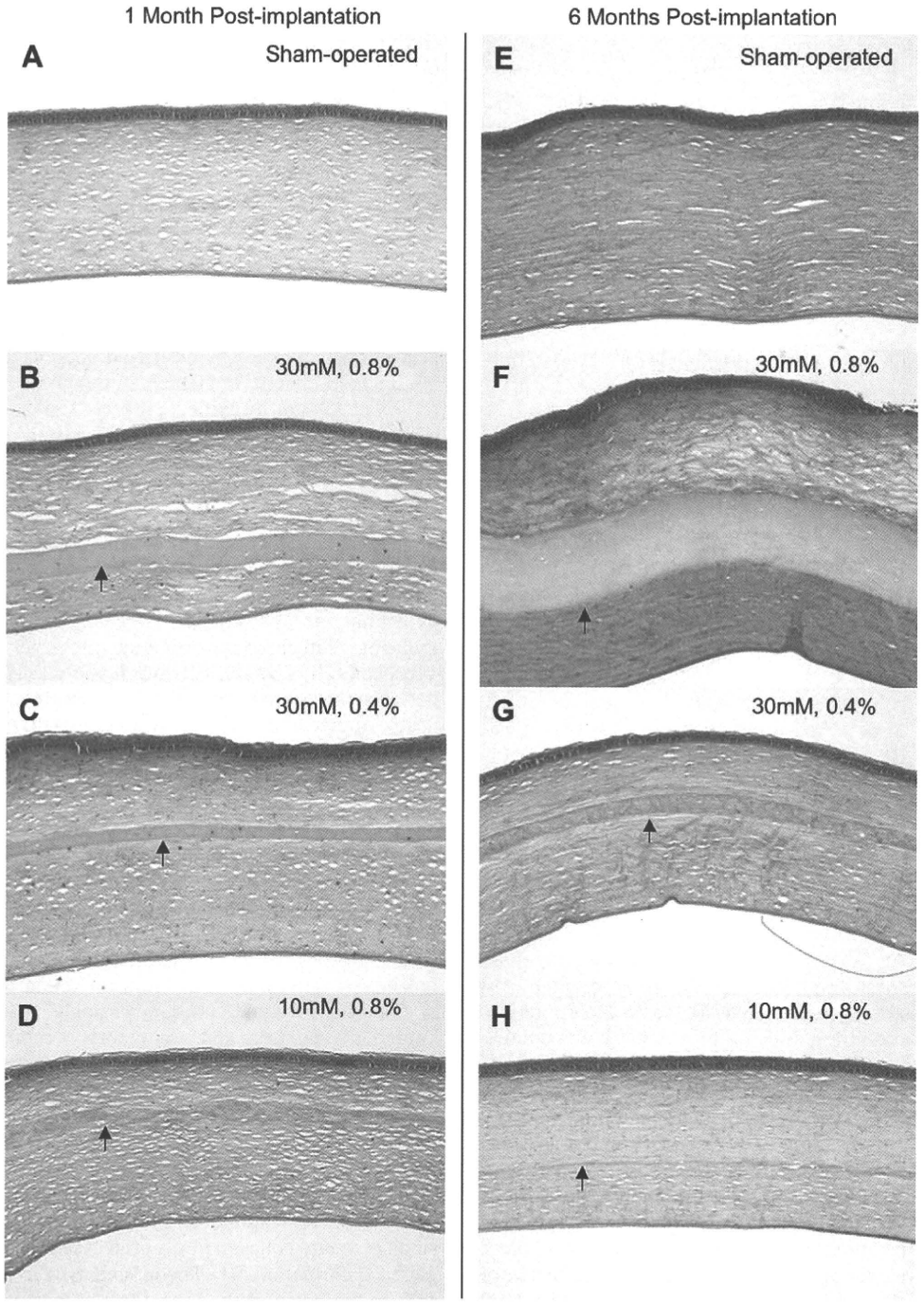


**Fig. 7.** 1 and 6 months post-implantation. Rabbit corneal cross sections with various collagen gels implanted into an intra-stromal pocket. Black arrows indicate the posterior surface of the implant. A: Control, B: 30 mM NaOH 0.8% EDC/NHS, C: 30 mM NaOH 0.4% EDC/NHS, D: 10 mM NaOH 0.8% EDC/NHS 1 month post-implantation. E: Control, F: 30 mM NaOH 0.8% EDC/NHS, G: 30 mM NaOH 0.4% EDC/NHS, H: 10 mM NaOH 0.8% EDC/NHS 6 months post-implantation.

to the formation of progressively condensing filamentous structures. At the lower pH levels, the condensing collagen filaments resembled the pathologically unraveling collagen fibrils that are found in necrotizing scleritis [43]. Higher pH levels resulted in the formation of tactoid-like structures [35] that possessed D-periodic banding. Similar results have been observed by other investigators, however, no fully mature collagen fibrils were observed in their studies [44]. *In vitro*, mature collagen fibrils that possess the characteristic D-banded periodicity occur when fibrillogenesis is carried out under greater pH levels [32,45–47].

The TEM images show that at NaOH levels above 40 mM, the filament structures within the gels demonstrate a high degree of compaction, and have associated into groups. Subsequently, the matrix of the gel appears considerably more heterogeneous. It may be that a fairly uniform refractive index within the gels was responsible for low levels of light scattering in the construct and the resultant good transparency. Loss of this ultrastructural uniformity might be responsible for the subsequent reduction in transparency.

Previous *in vivo* studies have shown that crosslinked collagen gels possess satisfactory biocompatibility for integration into

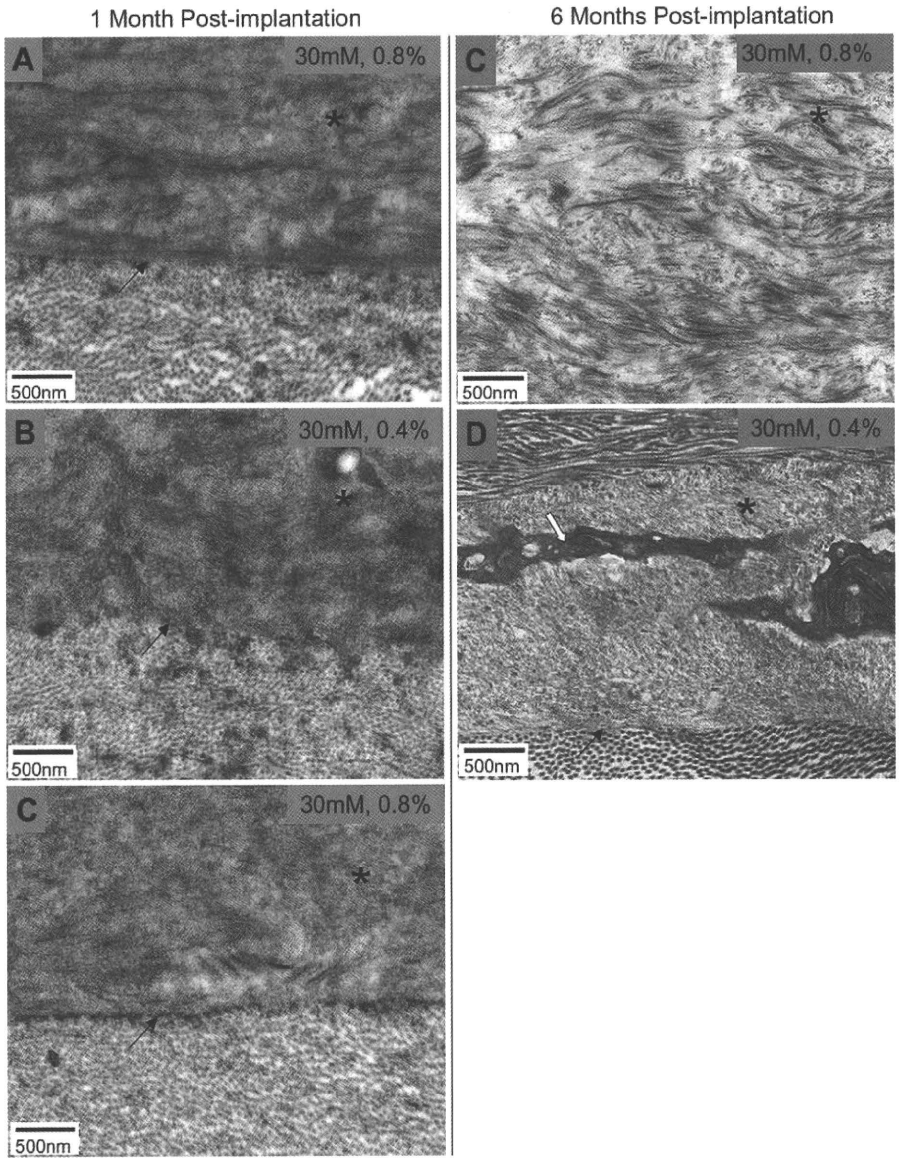


**Fig. 8.** 1 and 6 months post-implantation. TEM images at ×6000 magnification, of rabbit corneal stroma with various collagen gels implanted into an intra-stromal pocket. Before implantation the gel had a final collagen concentration of 10% (w/w).Asterisks indicates collagen gel implant. Black arrow indicates boundary between host stroma and gel implant. White arrow indicates invading host stromal cell. A: 30 mM NaOH 0.8% EDC/NHS, B: 30 mM NaOH 0.4% EDC/NHS at 1 month post-implantation. C: 30 mM NaOH 0.8% EDC/NHS, D: 30 mM NaOH 0.4% EDC/NHS at 6 months post-implantation.10 mM NaOH, 0.8% EDC/NHS gel was no longer present in the stroma at 6 months post-implantation.

stromal tissue and re-growth of host epithelial cells [32–34,48]. Our findings support the potential use of collagen-based constructs for clinical use as corneal stromal implants. The enhanced stability of the 30 mM NaOH, 0.8% EDC crosslinked gel within the intra-stromal pocket suggests that higher crosslinker levels, when coupled with greater levels of collagen fibrillogenesis, delay the digestion or degradation of the construct. However, the detrimental effect that these levels have on transparency of the gel must be taken into consideration. In addition, oedma in the anterior stroma suggests that the most stable gel (30 mM of NaOH, 0.8% EDC/NHS) may act as a barrier, preventing the endothelial pump from properly regulating anterior stromal hydration.

## 5. Conclusions

It is clear that within our constructs the assembly of type I collagen molecules can be manipulated over a wide pH range. In addition, even minor changes in the environmental conditions of the gels (such as pH), dramatically affects the optical and mechanical properties of the constructs. It was therefore necessary to establish a balance between the solution pH and crosslinker concentration. Nevertheless, whilst *in vitro* analysis can highlight the fundamental processes that govern fibrillogenesis, we must be careful to observe the limitations of any comparisons made to natural collagen assembly, as the complex arrangement of keratocytes and ECM macromolecules creates a unique and influential environment that cannot currently be replicated *in vitro. In vivo* implantation of the hydrogels into intra-stromal pockets demonstrated favourable biocompatibility, and highlighted the effect of higher levels of both fibrillogenesis and crosslinking on increased long term survival of the gels. Further work will be aimed at enhancing the optical and mechanical properties of the gels, and improving their long term *in vivo* characteristics through the addition of other ECM molecules. Presently, the optically transparent crosslinked collagen gels used in this study provide a basis for the future production of more complex biomimetic stromal

constructs utilizing orthogonally stacked layers of aligned collagen. The gels used in this study have potential clinical use as drug carriers, as protective membranes for corneal surface damage, and stromal implantation for tissue replacement and regeneration.

## Acknowledgements

We thank EPSRC (UK) and Global COE (Japan) for supporting this study. This work was supported in part by grants from the United Kingdom Engineering and Physical Sciences Research Council (Grant no. EP/F034970/1 to AJQ), the Grants-in-Aid for Scientific Research from the Ministry of Health Labor and Welfare, and from the Ministry of Education, Culture, Sports, Science, and Technology in Japan, and by the Tohoku University Global COE for conquest of Signal Transduction Disease with "Network Medicine". The authors confirm that there are no known conflicts of interest associated with this publication and there has been no significant financial support for this work that could have influenced its outcome.

## References

[1] Meek KM, Leonard DW. Ultrastructure of the corneal stroma: a comparative study. Biophys J 1993;64:273–80.
[2] Quantock AJ, Meek KM, Fullwood NJ, Zabel RW. Scheie's syndrome: the architecture of corneal collagen and distribution of corneal proteoglycans. Can J Ophthalmol 1993;28:266–72.
[3] Hogan MJ, Alvarado JA, Weddel JE. Histology of the Human Eye. Philadelphia: WB Saunders; 1971. pp. 55–111, 183–201.
[4] Komai Y, Ushiki T. The three-dimensional organization of collagen fibrils in the human cornea and sclera. Invest Ophthalmol Vis Sci 1991;32:2244–58.
[5] Ivarsen A, Fledelius W, Hjortdal JO. Three-year changes in epithelial and stromal thickness after PRK or LASIK for high myopia. Invest Ophthalmol Vis Sci 2009;50:2061–6.
[6] Hayashida Y, Akama TO, Beecher N, Lewis P, Young RD, Meek KM, et al. Matrix morphogenesis in cornea is mediated by the modification of keratan sulfate by GlcNAc 6-O-sulfotransferase. Proc Natl Acad Sci U S A 2006;103:13333–8.
[7] Henriksson JT, McDermott AM, Bergmanson JPG. Dimensions and morphology of the cornea in three strains of mice. Invest Ophthalmol Vis Sci 2009;50:3648–54.
[8] Müller L, Pels E, Vrensen G. The specific architecture of the anterior stroma accounts for maintenance of corneal curvature. Br J Ophthalmol 2001;85:437–43.
[9] Quantock AJ, Young RD, Tomoya AO. Structural and biochemical aspects of keratan sulphate in the cornea. Cell Mol Life Sci 2010;67:891–906.
[10] Maurice DM. The structure and transparency of the corneal stroma. J Physiol 1957;136:263–86.
[11] Hart RW, Farrell RA. Light scattering in the cornea. J Opt Soc Am 1969;59:766–74.
[12] Benedek GB. Theory and transparency of the eye. Appl Opt 1971;10:459–73.
[13] Birk DE, Fitch JF, Babiarz JP, Doane KJ, Linsenmayer TF. Collagen fibrillogenesis in vitro: interaction of types I and V collagen regulates fibril diameter. J Cell Sci 1990;95:649–57.
[14] Zhang G, Chen S, Goldoni S, Calder BW, Simpson HC, Owens RT, et al. Genetic evidence for the coordinated regulation of collagen fibrillogenesis in the cornea by decorin and biglycan. J Biol Chem 2009;284:8888–97.
[15] Lewis PN, Pinali C, Young RD, Meek KM, Quantock AJ, Knupp C. Structural interactions between collagen and proteoglycans are elucidated by three-dimensional electron tomography of bovine cornea. Structure 2010;18:239–45.
[16] Meek KM, Boote C. The use of X-ray scattering techniques to quantify the orientation and distribution of collagen in the corneal stroma. Prog Retin Eye Res 2009;28(5):369–92.
[17] Jester JV, Møller-Pedersen T, Huang J, Sax CM, Kays WT, Cavangh HD, et al. The cellular basis of corneal transparency: evidence for 'corneal crystallins'. J Cell Sci 1999;112:613–22.
[18] Jester JV. Corneal crystallins and the development of cellular transparency. Semin Cell Dev Biol 2008;19:82–93.
[19] Hu X, Lui W, Cui L, Wang M, Cao Y. Tissue engineering of nearly transparent corneal stroma. Tissue Eng 2005;11(11–12):1710–7.
[20] Orwin EJ, Borene ML, Hubel A. Biomechanical and optical characteristics of a corneal stromal equivalent. J Biomech Eng 2003;125:439–44.
[21] Ruberti JW, Zieske JD. Prelude to corneal tissue engineering – gaining control of collagen organization. Prog Retin Eye Res 2008;27(5):549–77.
[22] Germain L, Auger FA, Grandbois E, Guignard R, Giasson M, Boisjoly H, et al. Reconstructed human cornea produced in vitro by tissue engineering. Pathobiology 1999;67(3):140–7. LOEX.
[23] Griffith M, Hakim M, Shimmura S, Watsky M, Li F, Carlsson D, et al. Artificial human corneas: scaffolds for transplantation and host regeneration. Cornea 2002;2l(Suppl. 2):S54–61.
[24] Schneider AI, Maier-Reif K, Graeve T. Constructing an in vitro cornea from cultures of the three specific corneal cell types. In Vitro Cell Dev Biol Anim 1999;35(9):515–26.
[25] Tegtmeyer S, Papantoniou I, Muller-Goymann CC. Reconstruction of an in vitro cornea and its use for drug permeation studies from different formulations containing pilocarpine hydrochloride. Eur J Pharm Sci 2001;51 (2):119–25.
[26] Chen CS, Yannas IV, Spector M. Pore strain behaviour of collagen-glycosaminoglycan analogues of extracellular matrix. Biomaterials 1995;16 (10):777–83.
[27] Matsuda K, Suzuki S, Isshiki N, Yoshioka K, Okada T, Ikada Y. Influence of glycosaminoglycans on the collagen sponge component of a bilayer artificial skin. Biomaterials 1990;11(5):351–5.
[28] Osborne CS, Barbenel JC, Smith D, Savakis M, Grant MH. Investigation into the tensile properties of collagen/chondroitin-6-sulphate gels: the effect of crosslinking agents and diamines. Med Biol Eng Comput 1998;36(1):129–34.
[29] Yannas IV, Burke JF. Design of an artificial skin. I. Basic design principles. J Biomed Mater Res 1980;14(1):65–81.
[30] Tanaka Y, Kubota A, Matsusaki M, Duncan T, Hatakeyama Y, Fukuyama K, et al. Anisotropic mechanical properties in collagen hydrogels induced by uniaxial-flow for ocular applications. J Biomater Sci Polym Ed; 2010, [Epub ahead of print].
[31] Rafat M, Li F, Fagerholm P, Lagali NS, Watsky MA, Munger R, et al. PEG-stabilized carbodiimide crosslinked collagen–chitosan hydrogels for corneal tissue engineering. Biomaterials 2008;29(29):3960–72.
[32] Liu Y, Gan L, Carlsson DJ, Fagerholm P, Lagali N, Watsky MA, et al. A simple, crosslinked collagen tissue substitute for corneal implantation. Invest Ophthalmol Vis Sci 2006;47(5):1869–75.
[33] Liu Y, Griffith M, Watsky MA, Forrester JV, Kuffova L, Grant D, et al. Properties of porcine and recombinant human collagen matrices for optically clear tissue engineering applications. Biomacromolecules 2006;7(6):1819–28.
[34] Liu W, Merrett K, Griffiths M, Fagerholm P, Dravida S, Heyne B, et al. Recombinant human collagen for tissue engineered corneal substitutes. Biomaterials 2008;29(9):1147–58.
[35] Bard JB, Chapman JA. Polymorphism in collagen fibrils precipitated at low pH. Nature 1968;219:1279–80.
[36] Leibovich SJ, Weiss JB. Electron microscope studies of the effects of endo- and exopeptidase digestion on tropocollagen. A novel concept of the role of terminal regions in fibrillogenesis. Biochim Biophys Acta 1970;214 (3):445–54.
[37] Zeng Y, Yang J, Huang K, Lee Z, Lee X. A comparison of biomechanical properties between human and porcine cornea. J Biomech 2001;34(4):533–7.
[38] Crabb RA, Chau EP, Evans MC, Barocas VH, Hubel A. Biomechanical and microstructural characteristics of a collagen film-based corneal stroma equivalent. Tissue Eng 2006;12(6):1565–75.
[39] Christiansen DL, Huang EK, Frederick HS. Assembly of type I collagen: fusion of fibril subunits and the influence of fibril diameter on mechanical properties. Matrix Biol 2000;19(5):409–20.
[40] Roeder BA, Kokini K, Sturgis JE, Robinson JP, Voytik-Harbin SL. Tensile mechanical properties of three-dimensional type I collagen extracellular matrices with varied microstructure. J Biomech Eng 2002;124:214–22.
[41] Parry DA. The molecular and fibrillar structure of collagen and its relationship to the mechanical properties of connective tissue. Biophys Chem 1988;29 (1–2):195–209.
[42] Trelstad RL, Hayashi K, Gross J. Collagen fibrillogenesis: intermediate aggregates and suprafibrillar order. Proc Natl Acad Sci U S A 1976;73(11):4027–31.
[43] Watson PG, Young RD. Scleral structure, organisation and disease. A review. Exp Eye Res 2004;78(3):609–23.
[44] Harris JR, Reiber A. Influence of saline and pH on collagen type I fibrillogenesis in vitro: fibril polymorphism and colloidal gold labelling. Micron 2007;38 (5):513–21.
[45] Cisneros DA, Hung C, Franz CM, Muller DJ. Observing growth steps of collagen self-assembly by time-lapse high-resolution atomic force microscopy. J Struct Biol 2006;154(3):232–45.
[46] Gelman RA, Poppke DC, Piez KA. Collagen fibril formation in vitro. The role of the nonhelical terminal regions. J Biol Chem 1979;254(22):11741–5.
[47] Graham HK, Holmes DF, Watson RB, Kadler KE. Identification of collagen fibril fusion during vertebrate tendon morphogenesis. The process relies on unipolar fibrils and is regulated by collagen-proteoglycan interaction. J Mol Biol 2000;295(4):891–902.
[48] Merrett K, Liu W, Mitra D, Camm KD, McLaughlin CR, Liu Y, et al. Synthetic neoglycopolymer-recombinant human collagen hybrids as biomimetic crosslinking agents in corneal tissue engineering. Biomaterials 2009;30 (29):5403–8.

## Phakic Intraocular Lens for Keratoconus

Dear Editor:

Keratoconus is a progressive disorder that is characterized by central/paracentral thinning and protrusion of the cornea, causing myopic astigmatism. However, laser in situ keratomileusis is contraindicated for keratoconus eyes because it can induce keratectasia.[1] A phakic intraocular lens (PIOL) can be used to correct myopic astigmatism. The efficacy and safety of PIOL implantation for highmyopic has been studied.[2-5] Herein, we report the outcomes of iris-claw PIOL implantation in eyes with keratoconus.

The study protocol was approved by the institutional review board of the Minamiaoyama Eye Clinic. Thirty-six eyes of 24 patients (13 males and 11 females, 41.8±7.8 year old, −8.61 ± 3.21 D), who underwent PIOL implantation between May 2005 to December 2007, were enrolled. Thirty-two eyes were diagnosed as keratoconus and 4 eyes were diagnosed as pellucid marginal degeneration by videokeratography indices (TMS-IV, Tomey, Aichi, Japan; and OPD-10000, Nidek, Aichi, Japan). Patients with endothelial cell counts less than 1500/mm$^2$, anterior chamber depths less than 3.0 mm, previous eye surgeries, or other eye diseases were excluded. The toric 5/8.5 lens model was implanted in 15 eyes, the Artiflex 6/8.5 in 10 eyes, and the Myopia 6/8.5 in 11 eyes.

We performed a single laser iridotomy on the peripheral iris at 1 or 11 o'clock at least 1 week prior to the PIOL implantations. Corneoscleral incisions of 6.0 or 6.5 mm for implantation of ARTISAN Myopia or Toric lens models, or a 3.4-mm limbal incision for the Artiflex lens were centered at 12 o'clock. The PIOL was inserted into the anterior chamber, and fixed onto the midperiphery of the iris based on the manufacturer's instructions.

Postoperative examinations were performed on 1 day, 1 week, 1 month, 3 months, 6 months, and 1 year after surgery. For the statistical analysis, analysis of variance, a paired t test and Dunnett test were used. A $P$ value less than 0.05 was considered statistically significant.

Preoperative uncorrected visual acuity logarithm of the minimum angle of resolution (UCVA), 1.39±0.42, improved to 0.07±0.26 on 1 day, 0.04±0.20 at 1 week, 0.02±0.21 at 1 month after surgery, and showed no significant change thereafter ($P$<0.001 at all postoperative examination points; Fig 1; available at http://aaojournal.org). The best spectacle corrected visual acuity (BSCVA) at 1 year after surgery improved by 4 lines in 1 eye (2.8%), 2 lines in 4 eyes (11.1 %), 1 line in 9 eyes (25.0 %), unchanged in 19 eyes (52.8 %), and decreased 1 line in 3 eyes (8.3 %) from the preoperative value (Fig 2; available at http://aaojournal.org). The safety index (postoperative BSCVA/preoperative BSCVA) was 1.16±0.31 and the efficacy index (postoperative UCVA/preoperative BSCVA) was 0.87±0.31 at 1 year after surgery.

Preoperative manifest refraction (spherical equivalents), −8.38±3.42 D (−3.0 ~ −17.875 D) improved to −0.39±0.91 D (−3.75 ~ +2.00 D) at 1 week, −0.42±0.89 D (−3.625 ~ +2.00 D) at 1 month, and showed no significant change thereafter ($P$<0.001 at all postoperative examination points; Fig 3; available at http://aaojournal.org). Manifest refraction at 1 month postoperatively was within 0.5 D of the target refraction in 35 eyes (63.6 %), 1.0 D in 46 eyes (83.6 %), and 2.0 D in 53 eyes (96.4 %). Preoperative astigmatism, 2.44±2.25 D (0 D ~ 8.0 D), improved to 0.93±0.97 D (0 ~ 3.5 D) at 1 week, 0.62±0.69 D (0 ~ 2.5 D) at 1 month, and was stable thereafter.

Except for that 1 eye required resuturing of the wound 1 week after surgery because of wound recession, no intra- and postoperative complications were observed in the follow-up period. Intraocular pressure and central corneal endothelial count was stable and showed no significant change after surgery.

Approximately 86 % of patients answered "satisfied" or "very satisfied" with PIOL implantation at 1 year postoperative examination (Fig 4; available at http://aaojournal.org).

In summary, the 1 year results indicate that PIOL implantation for keratoconic eyes is predictable and effective, and PIOL implantation is one good means for correction of refractive error of keratoconus when BSCVA is not affected.

Naoko Kato, MD
Ikuko Toda, MD
Yoshiko Hori-Komai, MD
Chikako Sakai, BS
Hiroyuki Arai, MD
Kazuo Tsubota, MD
*Tokyo, Japan*

**References**

1. Comaish IF, Lawless MA. Progressive post-LASIK keratectasia: biomechanical instability or chronic disease process? J Cataract Refract Surg 2002;28:2206–13.
2. Asano-Kato N, Toda I, Hori-Komai Y, et al. Experience with the Artisan phakic intraocular lens in Asian eyes. J Cataract Refract Surg 2005;31:910–5.
3. Stulting RD, John ME, Maloney RK, et al; U.S. Verisyse Study Group. Three-year results of Artisan/Verisyse phakic intraocular lens implantation. Results of the United States Food And Drug Administration clinical trial. Ophthalmology 2008;115:464–72.
4. Tahzib NG, Nuijts RM, Wu WY, Budo CJ. Long-term study of Artisan phakic intraocular lens implantation for the correction of moderate to high myopia: ten-year follow-up results. Ophthalmology 2007;114:1133–42.
5. Güell JL, Morral M, Gris O, et al. Five-year follow-up of 399 phakic Artisan-Verisyse implantation for myopia, hyperopia, and/or astigmatism. Ophthalmology 2008;115: 1002–12.

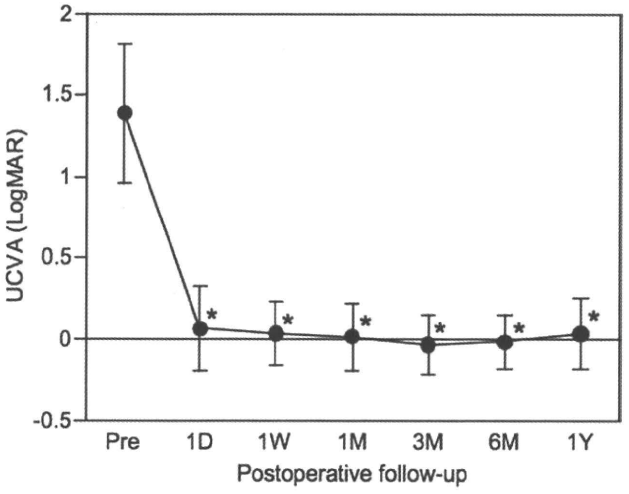


**Figure 1.** Changes in uncorrected visual acuity (UCVA) after phakic intraocular lens (PIOL) implantation. Uncorrected visual acuity (the logarithm of minimum angle of resolution) is significantly improved at 1 day after surgery, and stable until 1 year after surgery ($P < 0.001$ at all postoperative examination). D = day; M = month; W = week; Y = year. *$P < 0.05$ compared to the preoperative value.

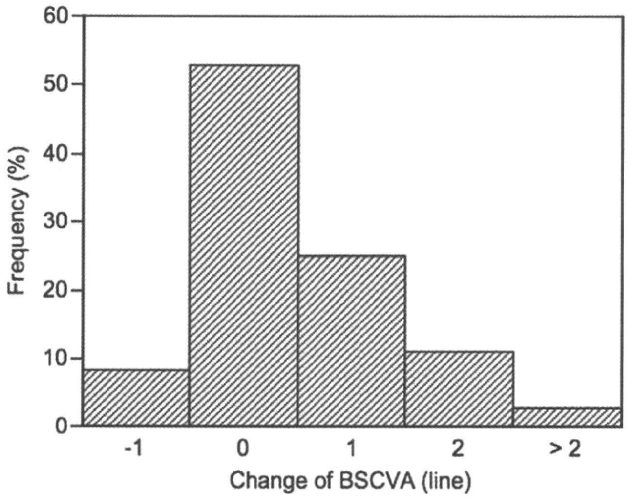


**Figure 2.** Changes in best corrected visual acuity (BSCVA) at 1 year after phakic intraocular lens (PIOL) implantation. The BSCVA improved more than 2 lines in 1 eye (2.8%), 2 lines in 4 eyes (11.1%), 1 line in 9 eyes (25.0%), was unchanged in 19 eyes (52,8%), and decreased 1 line in 3 eyes (8.3%).

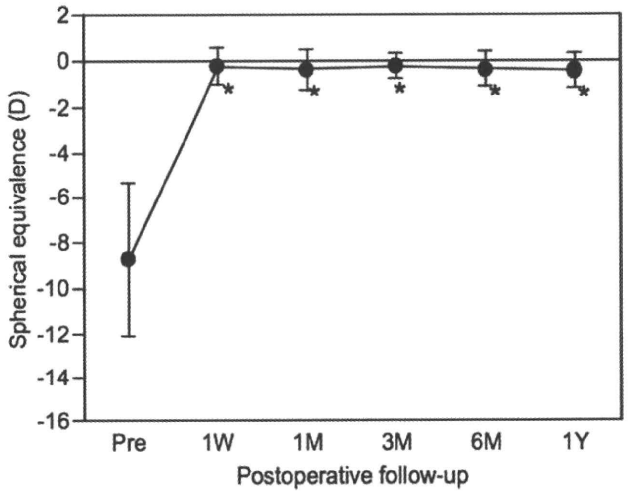


**Figure 3.** Changes in manifest refraction after phakic intraocular lens (PIOL) implantation. Manifest refraction is decreased shortly after surgery and stable up to 1 year ($P < 0.001$ at all postoperative examination points compared to preoperative value). *$P < 0.05$ compared to the preoperative value. W = week; M = month; Y = year.

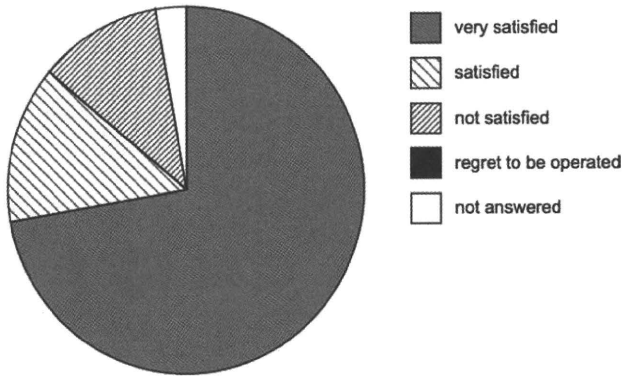


**Figure 4.** Patient satisfaction at the final examination points. Eighty-six percent of patients answered satisfied or very satisfied with phakic intraocular lens (PIOL) implantation at 1 year postoperative examination.

# Topography-Guided Conductive Keratoplasty: Treatment for Advanced Keratoconus

NAOKO KATO, IKUKO TODA, TETSUYA KAWAKITA, CHIKAKO SAKAI, AND KAZUO TSUBOTA

• PURPOSE: To evaluate the use of topography-guided conductive keratoplasty in eyes with keratoconus.
• DESIGN: Interventional case series.
• METHODS: We examined 21 eyes in 21 patients with advanced keratoconus. Topography-guided conductive keratoplasty was performed with intraoperative monitoring of corneal astigmatism using a surgical keratometer. Uncorrected visual acuity (UCVA), best spectacle-corrected visual acuity (BSCVA), corneal topography, manifest refraction, intraocular pressure (IOP), corneal endothelial cell counts, complications, and eventual outcomes were evaluated.
• RESULTS: UCVA (logarithm of the minimal angle of resolution [logMAR]), which was 1.65 ± 0.49 preoperatively, improved to 1.04 ± 0.64 at 1 week ($P < .001$) and 1.12 ± 0.61 at 1 month after surgery ($P < .001$). BSCVA, which was 1.02 ± 0.56 preoperatively, improved to 0.76 ± 0.65 at 1 week ($P = .026$) and 0.76 ± 0.60 at 1 month after surgery ($P = .003$). Manifest refraction, which was −15.13 ± 6.66 diopters (D) before surgery, declined to −9.97 ± 6.71 D at 1 month after surgery ($P = .002$). Although corneal topography reverted to the preoperative pattern and UCVA and BSCVA also regressed toward preoperative values, 12 of 21 eyes were better able to tolerate and conduct normal daily activities using contact lenses. Five subjects have undergone or are considering corneal transplantation after unsatisfactory postoperative results. No serious perioperative complication was observed.
• CONCLUSIONS: Topography-guided conductive keratoplasty may be effective in reshaping corneal configuration in eyes with keratoconus, without serious complications, and possibly contributed to avoiding or delaying corneal transplantation. (Am J Ophthalmol 2010;150:481–489. © 2010 by Elsevier Inc. All rights reserved.)

KERATOCONUS IS A PROGRESSIVE DISORDER CHARacterized by central or paracentral thinning and protrusion of the cornea. Keratoconus is usually diagnosed in the second or third decade of life, and as long as the disease is mild to moderate, the refractive error is typically corrected by wearing spectacles or contact lenses. However, as the disease progresses, correction with contact lenses becomes impossible in some patients.

Surgical approaches for advanced keratoconus have long been limited to corneal transplantation. Excimer laser–assisted corneal refractive surgery is relatively contraindicated for keratoconus eyes, because it can induce keratectasia postoperatively, resulting in more severe protrusion of the cornea, exacerbation of irregular astigmatism, and decreased visual acuity, especially after laser in situ keratomileusis.[1–3]

Recently, additional surgical options for keratoconus have been proposed. Corneal cross-linking, which is the instillation of riboflavin solution followed by ultraviolet A (UVA) irradiation, halts the progression of keratoconus.[4] Implantation of phakic intraocular lenses (IOL)[5] is also effective in the correction of refractive errors in eyes with keratoconus;[6,7] however, it is only appropriate for mild-to-moderate cases with good best spectacle-corrected visual acuity (BSCVA). The insertion of intracorneal ring segments can improve the uncorrected visual acuity (UCVA) of eyes with mild keratoconus and improve the BSCVA of eyes with moderate-to-advanced keratoconus.[8–13]

Conductive keratoplasty (CK)[14–16] is a novel method to reshape corneal configuration using radiofrequency energy. The efficacy of CK is attributed to the electrically conductive properties of the corneal stroma. The high-frequency energy is delivered to the cornea through a thin probe that penetrates 90% of the corneal stroma. The resistance to current flow through the tissue generates heat, resulting in a homogeneous thermal footprint, with controlled shrinkage of the surrounding collagen lamellae. For the correction of hyperopia or presbyopia, thermal spots placed on the mid-peripheral cornea cause a "belt-tightening" effect, which increases the curvature of the central cornea, inducing myopic shift.

The use of CK for modeling of the keratoconic cornea has previously been reported by 2 clinicians. Alió and associates[17] reported 3 cases of keratoconus or post-LASIK keratectasia that showed an improvement in visual acuity (1 or 2 lines) in response to CK, alone or in combination with intracorneal ring segments. Lyra and associates[18] reported treatment results for 25 eyes with keratoconus, in which 8 or 16 thermal spots were placed at 4.0 and 5.0 mm in the optical zone. The authors reported that BSCVA improved about 4 lines and manifest refraction improved 1 to

Accepted for publication May 13, 2010.

From the Department of Ophthalmology, School of Medicine, Keio University, Tokyo, Japan (N.K., T.K., K.T.); Minamiaoyama Eye Clinic, Tokyo, Japan (N.K., I.T., C.S.); and the Department of Ophthalmology, Nippon Medical School, Tokyo, Japan (N.K.).

Inquiries to Naoko Kato, Department of Ophthalmology, School of Medicine, Keio University, Shinanomachi 35, Shinjuku-ku, 160-8582 Tokyo, Japan; e-mail: naokato@sc.itc.keio.ac.jp

0002-9394/$36.00
doi:10.1016/j.ajo.2010.05.014

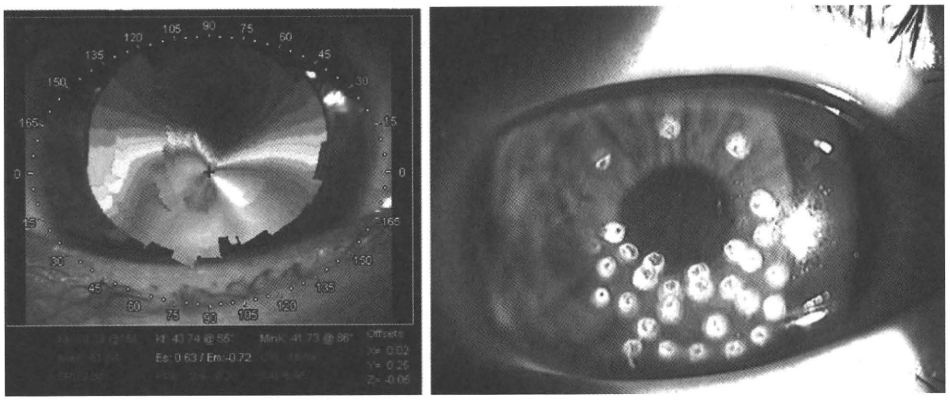

FIGURE 1. An example of topography-guided conductive keratoplasty for keratoconus. (Left) Thermal spots were placed according to preoperative corneal topography and intraoperative monitoring of corneal configuration, showing (Right) concentric reshaping in the inferior protruded area of the cornea.

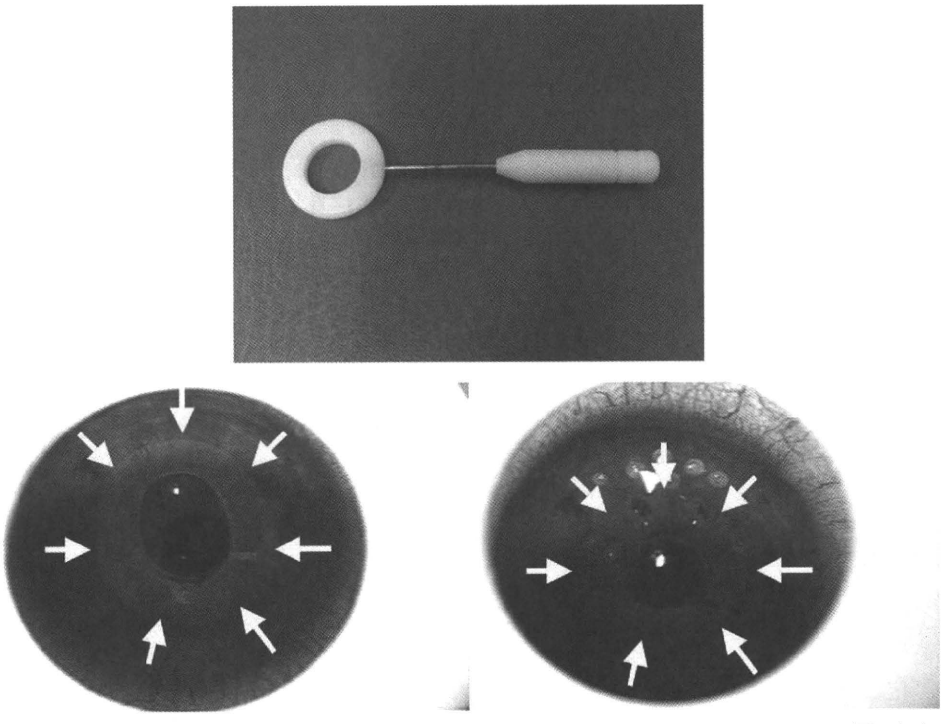

FIGURE 2. The keratoring for topography-guided conductive keratoplasty and its intraoperative use. (Top) A white ring with a handle was used to grossly assess the shape of the papillary area of the cornea during the surgery. The corneal shape was assessed by the reflex of the ring on the corneal surface. Note that (Bottom left) the white reflex (yellow arrows) of the ring is an ellipse before surgery, (Bottom right) becoming circular after topography-guided conductive keratoplasty.

3 diopters (D). Both investigators placed thermal footprints at regular intervals on the concentric ring in most cases.

We performed CK on the keratoconic cornea using a modified procedure. The tip of the delivery probe was placed more proximal to the pupillary center, approximately 3 to 5 mm in diameter. The pattern of application was modified according to the preoperative and intraoperative corneal shape. In most cases, the thermal footprints generated were concentrated in the inferior area of the cornea, where most of the protrusion occurs in the keratoconic cornea, resulting in flattening of the curvature and alignment of the cornea, according to individual corneal shape (Figure 1). We named this modified CK procedure topography-guided conductive keratoplasty. Topography-guided conductive keratoplasty was successful in reshaping the irregularity of advanced keratoconus quite effectively, reducing irregular astigmatism and improving visual acuity.

In this manuscript, we report our experience using topography-guided conductive keratoplasty for adva-

**TABLE.** Patients' Preoperative Profiles and Outcomes of Topography-Guided Conductive Keratoplasty

| Case | Age | Gender | Previous Surgery | Preop UCVA | Preop BSCVA | Preop MR | Preop Kave | Postop Best Achieved UCVA (Time After TGCK) | Postop Best Achieved BSCVA (Time After TGCK) | Postop Kave (Same Time Point as BSCVA) | Outcome at the Final Examination Point (Time of Final Evaluation) |
|---|---|---|---|---|---|---|---|---|---|---|---|
| 1 | 27 | M | — | 1.7 | 0.8 | −18.0 | 61.75 | 0.4 (1 wk) | 0.0 (6 mo) | 60.93 | CT (2 y) |
| 2 | 23 | M | — | 1.4 | 0.4 | −12.0 | 61.125 | 1.2 (1 d) | 0.2 (3 mo) | 52.5 | CL (1 y) |
| 3 | 17 | M | — | 0.4 | −0.1 | −12.0 | 49.875 | 0.5 (1 wk) | −0.1 (6 mo) | 46.125 | CL (1 y) |
| 4 | 28 | M | — | 1.7 | 1.0 | −9.0 | 50.625 | 0.2 (1 wk) | 0.0 (1 wk) | 43.125 | CL (1 y) |
| 5 | 32 | M | ICRS | 1.2 | 1.0 | −12.0 | 57.00 | 0.5 (1 wk) | 0.5 (1 wk) | 37.875 | (1 mo) |
| 6 | 42 | M | IOL | 1.3 | 1.0 | −23.0 | 68.875 | 1.1 (1 wk) | 0.8 (1 wk) | 54.755 | Repeated TGCK, CT (6 mo) |
| 7 | 20 | M | — | 1.7 | 0.7 | −10.0 | 44.02 | 1.0 (1 wk) | 0.7 (1 wk) | 32.155 | CT (6 mo) |
| 8 | 27 | M | — | 1.7 | 0.4 | −10.875 | 56.75 | 0.7 (1 d) | 0.0 (1 mo) | 49.215 | (6 mo) |
| 9 | 26 | M | — | 2.0 | 2.0 | 0 | 58.25 | 0.7 (1 d) | 0.4 (1 mo) | 57.5 | CL (3 mo) |
| 10 | 44 | M | — | 1.7 | 0.7 | −21.75 | 43.79 | 1.0 (1 wk) | 0.7 (1 mo) | 33.6 | Repeated TGCK, CL (1y) |
| 11 | 53 | M | — | 1.4 | 0.5 | −17.0 | 47.765 | 0.1 (1 wk) | 0.1 (1 wk) | 50.0 | (3 mo) |
| 12 | 19 | F | — | 1.4 | 0.4 | −6.5 | 62.425 | 0.1 (1 wk) | 0.1 (1 wk) | 49.25 | Repeated TGCK, CL (1y) |
| 13 | 45 | M | — | 2.0 | 1.4 | −14.0 | 62.935 | 1.4 (1 mo) | 0.3 (6 mo) | 52.33 | CL (1 y) |
| 14 | 45 | M | — | 2.0 | 1.7 | −28.5 | 52.105 | 2.0 (1 d) | 1.0 (1 y) | n.m. | CL (1 y) |
| 15 | 29 | M | — | 1.7 | 1.4 | −6.25 | 69.085 | 1.2 (1 d) | 1.5 (1 mo) | 53.485 | Repeated TGCK (6 mo) |
| 16 | 35 | M | — | 1.0 | 0.5 | −7.5 | 47.625 | 0.2 (1 mo) | 0.0 (1 wk) | 39.25 | CXL at 2 mo (1 y) |
| 17 | 48 | M | — | 2.0 | 1.5 | −18.0 | 47.95 | 2.0 (1 d) | 0.8 (3 mo) | 48.28 | Repeated TGCK, CT (6 mo) |
| 18 | 37 | M | IOL | 1.5 | 1.2 | −17.0 | 56.88 | 0.3 (6 mo) | 1.0 (1 wk) | 46.5 | CL (3 mo) |
| 19 | 28 | M | — | 1.7 | 1.7 | 0 | 39.05 | 0.8 (1 d) | 0.8 (1 wk) | 55.455 | CL, (CT) (3 mo) |
| 20 | 61 | M | — | 2.0 | 1.4 | −28.0 | 61.125 | 1.5 (1 d) | 1.3 (3 mo) | 64.24 | CT (1 y) |
| 21 | 27 | M | — | n.m. | 1.7 | −16.0 | n.m. | 1.7 (1 d) | 1.5 (1 wk) | 53.75 | CL (6 mo) |

BSCVA = best spectacle-corrected visual acuity; CL = performing normal daily activities with contact lenses; CT = corneal transplant; (CT) = waiting for corneal transplant; CXL = corneal cross-linking; d = day; F = female; ICRS = implantation of intracorneal ring segments; IOL = cataract extraction and intraocular lens implantation; Kave = average keratometric value; M = male; mo = months; MR = manifest refraction; n.m. = not measured; Postop = postoperative; Preop = preoperative; TGCK = topography-guided conductive keratoplasty; UCVA = uncorrected visual acuity; wk = week; y = year.

nced keratoconus, and we also discuss its indications and unsolved issues and possible solutions regarding this method.

## METHODS

• **PATIENTS:** Twenty-one eyes in 21 patients (20 male, 1 female; mean age, 34.7 ± 11.7 years; subjective refraction: −15.13 ± 6.66 D) with advanced keratoconus were enrolled. All patients were referred to or visited our institutes for corneal transplants because of extreme protrusion of the cornea and subsequently poor corrected visual acuity and/or contact lens intolerance. Two eyes had previously undergone cataract extractions and IOL implantations, and 1 eye had previously undergone the implantation of intracorneal ring segments.

• **KERATOCONIC CONDUCTIVE KERATOPLASTY PROCEDURE:** The ViewPoint CK System (Refractec, Inc, Irvine, California, USA) consists of a radiofrequency energy–generating console; a hand-held, reusable, pen-shaped hand piece attached to a removable cable and connector; a foot pedal that controls the release of radiofrequency energy; and a speculum that provides a large surface for the electrical return path.[15] A single-use, disposable, stainless-steel keratoplast tip is attached to the probe (Refractec, Inc); this tip delivers the current directly to the corneal stroma. The radiofrequency generator (RCS-200, Refractec, Inc) emits macropulses up to 1 second in duration. Each macropulse consists of micropulses, which are essentially 350-kHz sinusoidal waveforms. The amplitude of a set of micropulses is varied by changing the power setting on the CK unit. Typical clinical settings are 60% power (eg, 200 volt peak-to-peak) and 600-ms macropulse duration.

All surgeries were performed by the same surgeon (K. Tsubota), who was certified by Refractec, Inc. After the instillation of 4% xylocaine eye drops as topical anesthesia, the topography-guided conductive keratoplasty procedure was performed. The delivery probes were placed to make thermal spots, while simultaneously monitoring intraoperative changes using a keratoring (Handaya Co Ltd, Tokyo, Japan). The surgeon preplanned the spot placement pattern according to the topography map before surgery. Then, after making several initial spots, the surgeon examined the corneal configuration using the keratoring (Figure 2). When the configuration of keratoring was not